

## Article

# Optimizing Urban Mobility Through Complex Network Analysis and Big Data from Smart Cards

Li Sun , Negin Ashrafi  and Maryam Pishgar \*

Department of Industrial and Systems Engineering, University of Southern California, Los Angeles, CA 90089, USA; lsun4765@usc.edu (L.S.); ashrafin@usc.edu (N.A.)

\* Correspondence: pishgar@usc.edu

## Abstract

Urban public transportation systems face increasing pressure from shifting travel patterns, rising peak-hour demand, and the need for equitable and resilient service delivery. While complex network theory has been widely applied to analyze transit systems, limited attention has been paid to behavioral segmentation within such networks. This study introduces a frequency-based framework that differentiates high-frequency (HF) and low-frequency (LF) passengers to examine how distinct user groups shape network structure, congestion vulnerability, and robustness. Using over 20 million smart-card records from Beijing's multimodal transit system, we construct and analyze directed weighted networks for HF and LF users, integrating topological metrics, temporal comparisons, and community detection. Results reveal that HF networks are densely connected but structurally fragile, exhibiting lower modularity and significantly greater efficiency loss during peak periods. In contrast, LF networks are more spatially dispersed yet resilient, maintaining stronger intracommunity stability. Peak-hour simulation shows a 70% drop in efficiency and a 99% decrease in clustering, with HF networks experiencing higher vulnerability. Based on these findings, we propose differentiated policy strategies for each user group and outline a future optimization framework constrained by budget and equity considerations. This study contributes a scalable, data-driven approach to integrating passenger behavior with network science, offering actionable insights for resilient and inclusive transit planning.



Academic Editors: Hakilo Sabit and Peter Han Joo Chong

Received: 29 June 2025

Revised: 2 August 2025

Accepted: 4 August 2025

Published: 6 August 2025

**Citation:** Sun, L.; Ashrafi, N.; Pishgar, M. Optimizing Urban Mobility Through Complex Network Analysis and Big Data from Smart Cards. *IoT* **2025**, *6*, 44. <https://doi.org/10.3390/iot6030044>

**Copyright:** © 2025 by the authors. Licensee MDPI, Basel, Switzerland. This article is an open access article distributed under the terms and conditions of the Creative Commons Attribution (CC BY) license (<https://creativecommons.org/licenses/by/4.0/>).

**Keywords:** smart-card data; complex networks; network robustness; network characteristics analysis; transit optimization

## 1. Introduction

### 1.1. Background

Urban transportation strategies increasingly emphasize public transit as a core solution to congestion, supported by national policies promoting systems that meet evolving passenger needs [1]. As urban populations grow and travel patterns diversify, single-mode bus networks are proving inadequate. Cities are transitioning toward multimodal systems—such as Bus Rapid Transit (BRT) and trams—with differentiated operations and roles, forming integrated, dual-mode networks [2,3].

Technological advances, particularly smart-card fare systems, have enhanced transit services by capturing detailed boarding records. When integrated with GPS and transit management platforms, these systems facilitate real-time optimization of operations and resource allocation. However, data gaps remain—e.g., flat-fare policies omit alighting stations, limiting distance tracking [4]. Nevertheless, smart-card data remains invaluable

for analyzing demand distribution and usage behavior, especially in light of emerging flexible work schedules that continue to reshape transit needs [5].

Automated Fare Collection (AFC) systems record key transaction details, while Automated Vehicle Location (AVL) data enriches spatial analysis of bus stops and routes [6,7]. Leveraging these sources, this study investigates the behaviors and network impact of high-frequency (HF) and low-frequency (LF) passengers. HF users, such as commuters, often prioritize reliability and punctuality during peak hours, while LF users, including occasional riders and tourists, emphasize comfort and accessibility. Understanding these differences enables more targeted service strategies to improve system efficiency and user satisfaction.

Behavioral factors further influence transit mode choice—subjective perceptions of convenience, cost, and comfort are key determinants of travel behavior and policy compliance [8]. Identifying and addressing these nuances is essential for improving public transport's competitiveness with private modes.

Extensive research has leveraged big data to analyze public transit systems. Foundational work by Chen et al. utilized bus smart-card data to extract passenger flow patterns [9], followed by route-level indicators proposed by Daixiao et al. [10,11] and GIS-based enhancements by Zhu [12]. These studies established the analytical value of AFC data in operational planning. Building on these early efforts, researchers began integrating heterogeneous data sources to model travel behavior more comprehensively. At the system level, integrated platforms like Florida DOT's ADAMS consolidate AVL, APC, and AFC data for state-wide monitoring [13]. While ADAMS improved operations by consolidating data sources, it did not fully exploit cross-analysis for research insights. To bridge this gap, Barry et al. and Zhao [14,15] combined smart-card and GPS data to reconstruct travel trajectories and estimate OD matrices. Klein's work further introduced sensor fusion techniques such as Bayesian inference and neural networks to advance intelligent transit systems [16].

In parallel, research has increasingly focused on spatiotemporal travel behavior and the purposes behind transit usage. Chen et al. [17] identified simple versus complex trip chains to study mode selection, while Deng and Xiao [18] visualized peak-hour and off-peak spatial flow patterns. Other studies investigated temporal variability, including Wen's peak load prediction at transfer hubs [19] and Dong's analysis of non-work-related trips [20]. These efforts emphasized the importance of understanding dynamic and purpose-driven travel behavior.

To better capture user heterogeneity, clustering and segmentation techniques have been widely employed. Ali and Viallard [21,22] used K-means clustering to assess the stability of travel routines under varying conditions, such as holidays. Kieu [23] applied DBSCAN to identify groups with similar spatiotemporal behaviors. Yap [24] explored the elasticity of public transport demand, finding differential sensitivity across user groups, akin to Fulman et al.

Beyond user behavior, another body of work applies complex network theory to analyze public transit system structures. Gao and Wu [25] demonstrated scale-free and small-world properties in Beijing's bus network, findings consistent with Derrible and Kennedy's metro studies across global systems [2]. Wang and colleagues extended this approach to other cities, while Yan applied it to non-motorized networks in Xi'an [26], reinforcing the utility of network theory in diverse contexts. Building on these structural insights, more recent studies have examined resilience and vulnerability in transit networks. Miao et al. proposed an accessibility-based framework to evaluate the impact of station or link closures on urban connectivity [27]. Da Silva analyzed network inefficiencies and congestion patterns in Curitiba's BRT system [28]. Yap and Cats [29] incorporated machine learning with network measures to predict disruptions and identify high-risk stations

for targeted intervention. In the context of sustainable transit planning, Wenz et al. [30] proposed a route prioritization methodology to facilitate the transition from conventional buses to electric buses. Similarly, Chen et al. [31] developed a lane-changing trajectory extraction and classification framework based on large-scale empirical data, supporting microscopic traffic flow modeling. Zhou et al. [32] applied spatial syntax and OD simulation to evaluate the coupling between road network saturation and spatial structure, offering topology-aware insights for traffic planning. Lyu et al. [33] further integrated trajectory data with network analysis to quantify urban road efficiency and inform function-oriented transport network design.

Despite the breadth of existing literature, most prior research either focuses on aggregated transit behavior or analyzes structural properties without differentiating user groups. Moreover, the dynamic interactions between heterogeneous passengers and network topology remain underexplored. These limitations underscore the need for more granular, behavior-aware analyses that integrate spatiotemporal data with network science. The following section outlines the key research gaps and theoretical contributions addressed in this study.

### 1.2. Research Gaps and Contributions

Building on the foundation of prior work, this study aims to advance the understanding of urban transit systems by filling several critical gaps in the literature:

- Lack of frequency-based user differentiation: Existing studies rarely distinguish between high- and low-frequency travelers, despite their differing contributions to peak-hour congestion, network robustness, and spatial flow distribution. This limits our understanding of demand heterogeneity within the transit system.
- Insufficient exploration of dynamic network behaviors: Most prior work analyzes static topological structures, overlooking temporal variations, peak-valley transitions, and disruption responses. The dynamic, multilayer nature of real-world urban transit networks remains underexplored.
- Limited integration of large-scale smart-card and GPS data with network science: Although AFC and AVL data are widely collected, few studies systematically integrate them to reveal structural vulnerability, community flow patterns, and route centrality based on real passenger behavior.

To address these gaps, this study proposes a novel framework that combines large-scale AFC and AVL datasets with advanced complex network analysis. By classifying and comparing high- and low-frequency passengers, and modeling their behaviors across time, space, and network structure, this study provides five key contributions to the analysis and planning of large-scale multimodal urban transit networks:

- A data-driven perspective on how different user groups shape network load, congestion risks, and robustness, revealing distinct behavioral impacts from high-frequency and low-frequency travelers;
- A scalable methodology for identifying critical nodes, vulnerable sub-networks, and modular communities in dual-mode transit systems using smart-card data and complex network indicators;
- A policy-relevant framework for assessing transit equity and resilience, capable of supporting infrastructure planning and vulnerability mitigation in response to disruptions. The distinction between centralized but fragile high-frequency networks and dispersed but resilient low-frequency networks offers practical guidance for building more inclusive and robust urban mobility systems;
- A foundational framework for future optimization: although this study does not directly solve optimization problems, it identifies structural vulnerabilities—such as

low-redundancy links, fragile subnetworks, and centrality-induced bottlenecks—that can guide future algorithmic development.

## 2. Methodology

To analyze the structural and behavioral differences between HF and LF passenger groups, we design a six-step methodological framework as shown in Figure 1. Each step contributes a specific function in transforming raw smart-card records into meaningful insights for network assessment and planning.

**Step 1: Data Preprocessing.** The goal of this step is to construct reliable and continuous travel chains from raw smart-card data. We extract detailed records covering both subway and bus modes, remove incomplete or duplicate entries, and ensure that each passenger's travel chain is temporally and spatially coherent. This ensures high data integrity for subsequent frequency classification and network construction.

**Step 2: Station Clustering.** Given the spatial complexity of Beijing's transit system—comprising over 53,000 unique stations—we apply the K-means clustering algorithm to group stations based on geographic coordinates (latitude and longitude). This process reduces network dimensionality and facilitates tractable analysis by transforming the raw stop-level data into 537 representative cluster nodes, preserving key spatial patterns while improving model scalability.

**Step 3: Travel Frequency Classification.** In this step, we categorize passengers into HF and LF groups based on their total number of valid trips during the observation period. This classification enables the construction of differentiated network models and supports targeted analysis of how rider behavior impacts system load, robustness, and congestion.

**Step 4: Complex Network Model Construction.** We construct two directed, weighted graphs—one for HF travelers and another for LF travelers—based on their observed trips between clustered station nodes. These networks encode temporal and spatial travel behaviors into a topological structure, with edges representing directed passenger flows and weights reflecting trip volumes.

**Step 5: Network Visualization.** To aid interpretation, we generate visual representations of the HF and LF networks. These diagrams reveal traffic distribution, highlight major transfer corridors, and illustrate inter-community flow differences. Visualization provides an intuitive understanding of mobility patterns and network usage disparities across traveler types.

**Step 6: Network Characteristics Analysis.** This step offers a multifaceted examination of network structure and dynamics:

- **6.1 Node Characteristics:** We analyze node-level metrics including degree, betweenness centrality, and closeness centrality to identify key transit hubs and their functional importance in network connectivity and load distribution.
- **6.2 Robustness Test:** We simulate node removal scenarios—both random and targeted—to evaluate each network's vulnerability to disruption and identify critical weak points in the HF and LF networks.
- **6.3 Basic Network Properties:** We assess global properties such as degree distribution, average path length, clustering coefficient, and global efficiency to understand structural cohesion and operational potential.
- **6.4 Community Detection:** Using the Louvain algorithm, we identify modular substructures and analyze inter- and intra-community flow, which reflect the spatial organization of rider activity.
- **6.5 Peak Hour Analysis:** We isolate travel data during peak periods to evaluate how congestion affects network performance and passenger flow distribution, offering insights into time-sensitive vulnerabilities.

This step-by-step framework supports a scalable, behavior-sensitive approach to analyzing transit network dynamics, forming the foundation for policy recommendations and future optimization modeling.

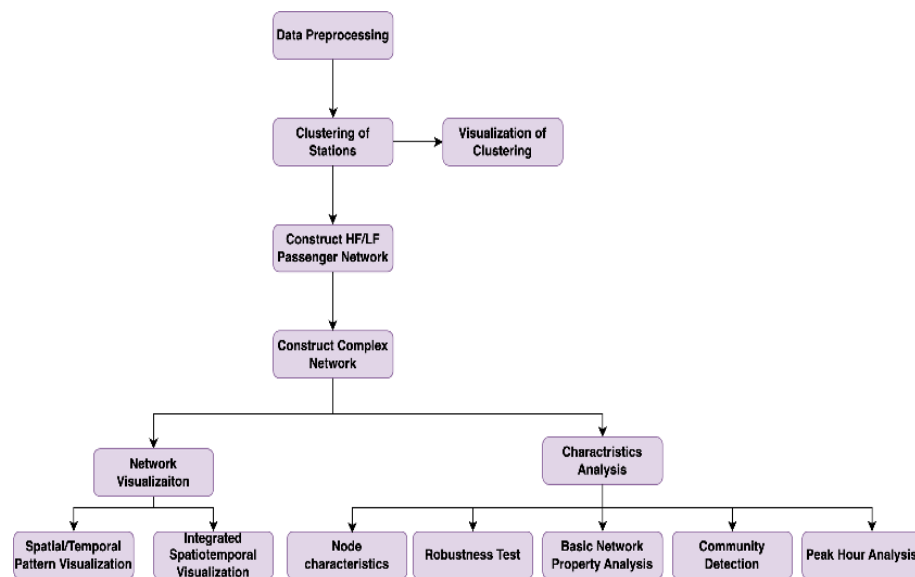


**Figure 1.** Flowchart of data preprocessing, clustering, and network analysis processes. Each arrow represents the sequential progression of analytical steps, rather than the transfer of information between stages.

### 3. Research Data Pre-Processing

#### 3.1. Introduction to Public Transportation Data

The primary sources of public transport big data, including smart-card data and station data from buses and subways, are often distributed across different systems with varied data formats. Given the diversity of these data sources and the inconsistency in formats, data preprocessing becomes crucial in ensuring the effectiveness of the research.

In related work by Ma Yiqing [34], smart IC card data emerges as a critical source, offering detailed insights into passenger interactions within the transport system. A deep dive into these details enables a nuanced understanding of passenger travel behaviors. For instance, Table 1 provides a thorough explanation of each field in the IC card dataset. In focusing on the primary objectives of this study, data elements that do not directly impact the research outcomes, such as expenditure amount, remaining balance, and transaction type, are excluded from the data extraction process. This selective approach to data handling sharpens the research focus and enhances the efficiency and accuracy of data processing.

**Table 1.** IC card data segments.

Field Name	Data Type	Explanation
BUSNO	Varchar2	Vehicle Code
CARDNO	Varchar2	Card Number
CONSUME	Number	Amount Spent
CONSUMEDATE	Date	Transaction Time
CONSUMETYPE	Number	Transaction Type
LINENO	Varchar2	Line Code
REMAINTIMES	Number	Remaining Times

### 3.2. Research Data

In this study, the data structure is meticulously designed to comprehensively capture and represent the travel characteristics of passengers within the transit system. As illustrated in Table 2, the data structure meticulously logs the travel activities of passengers. This includes an encrypted passenger identifier, the bus or subway line number, the sequence number and name of the boarding station on that specific line, and the precise time of card swiping, enriching the temporal dimension of the passengers' travel patterns.

**Table 2.** Passenger records of travel segments.

Passenger ID	Mode	Line	Station	Station Name	Time	Next Chain
770fdeffe6154df9a2f631027035	DT	6	49	Jintai Road	20180301090700	DT
770fdeffe6154df9a2f631027035	DT	14	67	Dawang Road	20180301143200	DT
770fdeffe6154df9a2f631027035	GJ	423	10	Xinfadi Bridge West	20180301164301	GJ
770fdeffe6154df9a2f631027035	GJ	22	1	Mudanyuan	20180301185301	GJ
7ef24c978d18195279f53c5a0b3	DT	6	57	Huangqu	20180301123900	DT
770fdeffe6154df9a2f631027035	DT	6	49	Jintai Road	20180301090700	DT

For passengers engaging in transfers, the structure goes further to document the exact time of the transfer and details of the subsequent travel chain. This includes the sequence number of the transfer station and the time of transfer, thereby compiling a complete record of the passenger's travel route.

It is crucial to acknowledge the immense volume of data handled in this analysis—approximately 18 million rows of passenger travel records daily over a span of 14 days, culminating in about 20 million rows of data in total. Among these records, subway-related trips (including both subway-only and combined bus-subway journeys) account for approximately 65%, while bus-related trips account for about 35%. Notably, around 20% of all travel chains involve both bus and subway segments, reflecting the high prevalence of multi-modal commuting behavior in Beijing's transit system. These blended journeys not only highlight the integrated nature of the network but also introduce additional complexity in modeling and analysis. As such, careful preprocessing and segmentation are essential to ensure analytical accuracy and relevance.

As presented in Tables 3 and 4, the longitude and latitude of the stations provide essential spatial information for analyzing the geographical structure of the transit network. Rather than focusing solely on the precise location of individual stations, these coordinates are primarily used to calculate inter-station distances, which form the basis for exploring network characteristics such as connectivity, clustering coefficients, and shortest paths.

**Table 3.** Subway Station Coordinates.

Station Name	Longitude	Latitude
Anhe Bridge North	116.269956	40.012195
Beiyuan	116.277647	40.002373
Guoyuan	116.290908	39.998258
Yuanlingyuan	116.310186	39.999662
Peking University East Gate	116.315842	39.992212
Shuguang Road	116.316467	39.983991
Haidian Huangzhuang	116.317564	39.975996

**Table 4.** Bus station coordinates.

Station Name	Longitude	Latitude
Tiantongyuan	116.3465167	40.00291006
Tiantongyuan Bridge West	116.338111	39.89619858
Xiaoying	116.328866	39.89615096
Huanggang Village South Entrance	116.5236192	39.92578004
Dongbei Wang Middle Road	116.2855868	40.03777604
Hongfu Industry Garden	116.500131	39.801502
Liangxiang Bus Station	116.527203	39.92557497

Moreover, the availability of geographical coordinate data facilitates the creation of visual representations. Using MATLAB R2024a or similar visualization tools, station flow diagrams can be developed to illustrate the usage of individual stations and the movement patterns of passengers between different stations across the city. These visualizations offer valuable insights into spatial and temporal travel behaviors, aiding in identifying key transit hubs and optimizing the overall transportation network.

### 3.3. Passenger Data Preprocessing Methodology

The raw smart-card dataset contained over 26 million records and required systematic preprocessing to ensure analytical reliability. The following automated filtering procedures were applied:

1. **Duplicate Record Removal:** Records were classified as duplicates if they had identical card ID, boarding time (to the minute), route ID, and boarding/alighting stations. These entries were removed using a hash-based deduplication process implemented in Python 3.10.
2. **Anomaly Detection and Filtering:** Entries with abnormal durations (e.g., <1 min or >240 min), trips exceeding 50 km in inferred distance, or illogical time order (boarding after alighting) were removed. Thresholds were empirically determined based on percentile distributions across the full dataset.
3. **Incomplete Travel Chain Identification:** A trip was considered incomplete if any of the key fields (e.g., alighting station, route ID) were missing or inconsistent. These were filtered using rule-based logic scripts. Approximately 20% of records were excluded under this step.

These procedures reduced noise and inconsistency, resulting in a clean dataset of 20 million valid trips. This curated dataset forms the foundation for network construction, clustering, and robustness evaluation.

### 3.4. Station Clusters

Due to the complexity of passenger and site information, direct visualization often yields suboptimal results. To address this challenge, a clustering algorithm is applied to process site information, enabling the extraction of more meaningful patterns. The motivation for employing K-means clustering in this study lies in its ability to reduce data complexity and enhance computational and analytical efficiency. By aggregating a large number of individual sites into a smaller number of representative cluster nodes, the analysis not only becomes more manageable but also facilitates the identification and understanding of key nodes and connections within the urban transportation network.

In this study, the K-means clustering algorithm is employed due to its widespread use and effectiveness. The algorithm operates by dividing the dataset into K clusters, minimizing the sum of distances from each data point to its nearest centroid. The process begins with the random selection of K data points as initial centroids. Through iterative refinement,

each data point is assigned to the nearest centroid cluster, followed by an update of the centroid positions based on the newly assigned clusters. This iterative process continues until convergence conditions are met, either when centroid updates no longer significantly change the clusters or when a preset number of iterations is reached. This approach ensures a systematic reduction of complexity while retaining critical insights into the network's structure and dynamics.

To determine a suitable number of clusters, we conducted an Elbow Method analysis by calculating the within-cluster sum of squares (WCSS) across a range of  $K$  values. The resulting curve showed a distinct inflection point near  $K = 537$ , suggesting this as an appropriate choice that balances model simplicity with clustering quality. This selection also aligns with practical considerations, as it approximates the number of administrative subdistricts in Beijing and maintains sufficient spatial granularity for subsequent analysis.

In this study, a mixed clustering approach was applied to 53,700 subway and bus stations, ultimately grouping them into 537 nodes. This method effectively simplifies the network model while preserving critical traffic flow information, making it feasible to conduct more focused and efficient network analysis and optimization. By reducing the complexity of the data, this clustering process ensures that the essential structural and operational characteristics of the transportation network are retained.

The results of the clustering process highlight the key nodes in the network, as partially shown in Table 5, with the detailed stations belonging to the first cluster center presented in Table 6. It is important to note that bus and subway stations were clustered together in this analysis. Despite their differences, this mixed clustering approach does not compromise the accuracy or effectiveness of the clustering results, demonstrating its robustness and suitability for analyzing integrated urban transportation networks.

**Table 5.** The central node after clustering.

Clustering Nodes	Latitude	Longitude
0	40.04867448	116.4066763
1	40.44167793	115.9061828
2	39.854609	116.3362191
3	40.35755938	116.5678062
4	39.97114007	115.9879883
5	39.87181985	116.6642087

**Table 6.** The first cluster center internal site.

Stop Number	Stop Name	Longitude	Latitude	Node Number
42388	Xisan Village	116.5894841	40.36254838	0
42399	Xisan Village	116.5898399	40.36246982	0
42400	Koutou	116.570183	40.36211652	0
42547	Guanhe Crossing	116.554231	40.36048595	0
42548	Sanhe Crossing	116.5489953	40.37759114	0
42581	Beizhai Village East	116.5588375	40.336021	0

During the clustering process, the new centroid of each node is determined by calculating the mean of all sites belonging to the cluster. This includes averaging the longitude and latitude of the sites and summing their respective traffic flows. Consequently, the position of each node represents the geometric center of all sites within the cluster, while the node's traffic reflects the cumulative flow of these sites. Additionally, the inter-station traffic data is standardized using a maximum-minimum normalization approach after clustering.

This approach ensures that the longitude, latitude, and flow data of each node not only capture the spatial distribution of traffic but also provide insights into the degree of traffic aggregation within the network. By combining spatial and flow characteristics, this method enhances the understanding of network dynamics and facilitates the analysis of inter-node interactions. The clustering results, including inter-node flow data, are summarized in Table 7.

**Table 7.** Inter-node flow rate after clustering.

Start-Site Node ID	Terminating-Site Node ID	Start-Site Longitude	Start-Site Latitude	Terminating-Site Longitude	Terminating-Site Latitude	Flow	Standardized Traffic
121	234	116.453518	39.9081348	116.470691	39.91255031	56,811	1
234	121	116.470691	39.91255031	116.453518	39.9081348	51,013	0.897940503
121	42	116.453518	39.9081348	116.630711	39.89759435	37,126	0.653494103
234	144	116.470691	39.91255031	116.7877687	39.9473497	33,524	0.5908098773
234	470	116.470691	39.91255031	116.498658	39.91021268	31,525	0.5549023063
245	234	116.4698259	39.93250931	116.470691	39.91255031	29,423	0.517910778
245	234	116.470691	39.91255031	116.4698259	39.93250931	29,378	0.517910664
470	234	116.498658	39.91021268	116.470691	39.91255031	28,940	0.509397513
121	7	116.453518	39.9081348	116.4569124	39.89013758	28,234	0.496972364
7	121	116.4569124	39.89013758	116.453518	39.9081348	28,160	0.495669776

This study undertakes a comprehensive preprocessing of intelligent IC card data for buses and subways, urban road network data, and the location information of bus and subway stations in Beijing for March 2018. The preprocessing steps include removing duplicate records, correcting incomplete travel chains, and excluding records with obvious defects, thereby ensuring the quality and accuracy of the data for subsequent analysis. Additionally, the structure of the dataset is carefully outlined, encompassing fields such as passenger ID, transportation mode or route, station number and name, travel time, and subsequent travel chain details. These fields provide essential information for analyzing passenger travel patterns.

### 3.5. Section Summary

The dataset comprises approximately 1,800,000 daily records spanning 14 days, totaling nearly 200,000,000 records, offering a robust basis for this research. Latitude and longitude information for 288 subway stations and 53,443 bus stations in Beijing is collected and processed, providing a physical spatial foundation for analyzing inter-station traffic and complex network characteristics. This spatial data also enables the visualization of traffic flows. To further simplify the network model, the K-means clustering algorithm is employed to cluster 53,700 subway and bus stations into 537 nodes. This method effectively reduces data complexity while preserving critical traffic flow information, facilitating detailed network analysis and optimization.

The preprocessing efforts establish a strong data foundation, supporting the analysis of high- and low-frequency travel modes, complex network characteristics, and the formulation of service optimization strategies in subsequent analyses.

## 4. Network Construction

### 4.1. High and Low Frequency Passenger Networks

This study successfully constructs a daily travel chain information database for bus passengers through in-depth mining and analysis of big data from the public transportation system. The database utilizes a unified storage format, organizing the data based on passengers' IC card numbers, thereby forming a structured and extensive database of bus travel chain information. Within this system, it becomes straightforward to retrieve the

complete travel trajectory of any passenger on a specific date and perform detailed analyses of the spatiotemporal distribution characteristics of transit travel.

In addition to the creation of this extensive bus travel chain database, the study also emphasizes the development of high and low-frequency passenger networks. By distinguishing passengers based on their travel frequency, two distinct sub-networks are formed: one for high-frequency passengers who use public transportation regularly, and another for low-frequency passengers who infrequently rely on the bus system. This differentiation facilitates a more detailed examination of passenger travel behaviors and provides targeted data to support the precise planning and optimization of the bus network. The aim of constructing these high and low-frequency passenger networks is to better understand the travel patterns and needs of different passenger groups. This insight is crucial for developing more efficient, personalized operational strategies, enhancing service quality, and contributing to the sustainable development of urban public transportation systems.

Each step was designed to improve the accuracy and effectiveness of the data analysis, ensuring a robust and reliable dataset for subsequent analysis. These steps are comprehensively illustrated in Figure 2, which provides a visual representation of the detailed process.

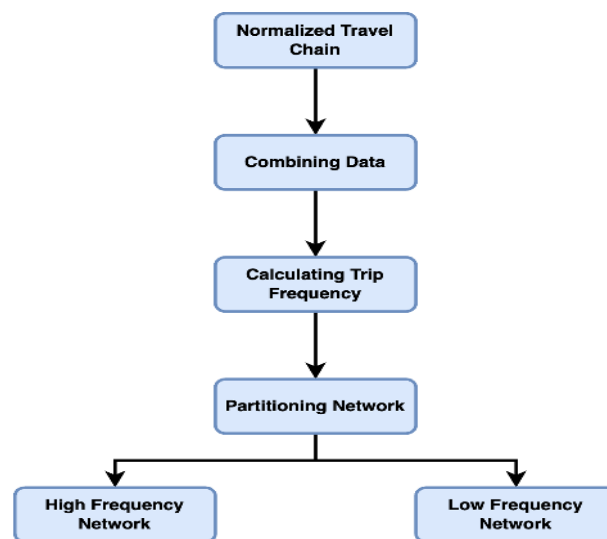


**Figure 2.** A GIS diagram of bus stops and subway stations.

**Step 1—Standardization of Travel Chains:** The bus data includes multiple fields for each passenger's travel information, such as travel mode, route number, station number, station name, and card swiping time. To simplify the analysis, these fields were integrated into standardized travel chain units by grouping every five fields together, following the passenger ID. This process not only simplified the data structure but also ensured the completeness and clarity of each travel chain. The standardized travel chains are shown in Table 8.

**Step 2—Merging Data:** All passenger data within a week was merged and reorganized based on the passenger ID. This consolidation was essential for enabling more efficient data processing in the subsequent analysis.

**Step 3—Determining Travel Frequency:** The core of this step involved calculating each passenger's travel frequency within the week. By counting the number of times each passenger ID appears in the dataset per day, the study accurately determined the travel frequency for each passenger over the course of the week.

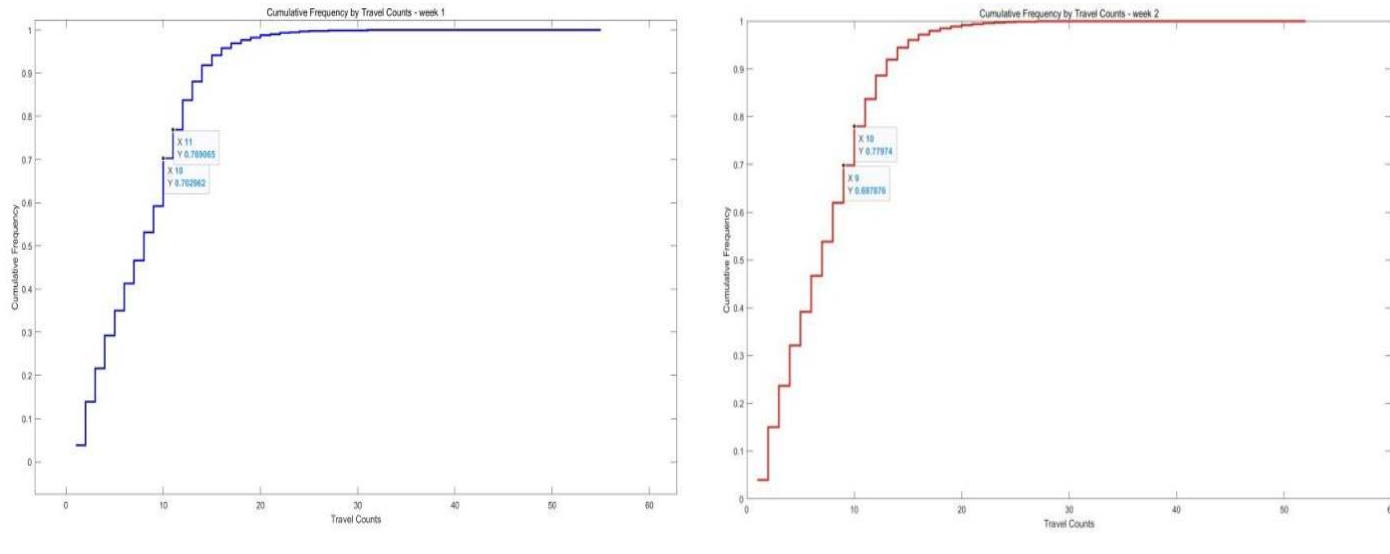
**Step 4—Determining the Division Threshold:** Through a comprehensive analysis of travel data, the distribution characteristics of travel frequencies were assessed. The study tallied the number of trips and cumulative frequencies over a two-week period, observing

the disparity in travel frequencies between high- and low-frequency passengers. Figure 3 illustrates these findings, where the X-axis represents the number of trips (i.e., individual travel counts per passenger), and the Y-axis represents the cumulative proportion of passengers—that is, the proportion of all users whose travel frequency is less than or equal to the corresponding value on the X-axis. This cumulative distribution helps to reveal the skewness in passenger travel behavior and serves as the basis for selecting a threshold to distinguish between high- and low-frequency travelers.

**Step 5—Dividing High and Low Frequency Passenger Networks:** In the absence of a clear natural boundary in cumulative travel frequencies, a threshold of approximately 25% was selected. Passengers with the highest 25% of travel frequencies were classified as high-frequency passengers, while the rest were categorized as low-frequency passengers. Passengers traveling 11 or more times in the first week and 10 or more times in the second week were designated as high-frequency, while all others were classified as low-frequency. The resulting high- and low-frequency passenger networks are presented in Tables 9 and 10.

**Table 8.** Passengers' travel chains.

Passenger ID	Travel Chain1	Travel Chain2	Travel Chain3
78aa216c934e339e650f119ced	DT, 1, 24, SiHui, 20180301065200	DT, BatongLine, 11, Liyuan, 20180301072757	
78aa216c934e339e650f119ced	DT, 1, 24, SiHui, 20180301082500	DT, BatongLine, 9, Guoyuan, 20180301084903	
78aa216c934e339e650f119ced	DT, 6, 53, Qingnianlu, 20180301094300	DT, 6, 57, Huangqu, 20180301095108	
78aa216c934e339e650f119ced	GJ, 675, 12, Dougezhuanglu, 20180301103001	GJ, 675, 17, QingnianluKou, 20180301103911	GJ, 2, 10, Shilibu, 20180301104601
78aa216c934e339e650f119ced	DT, 6, 51, Shilibu, 20180301120000	DT, 6, 69, BeiyunheWest, 20180301123014	
78aa216c934e339e650f119ced	GJ, 648, 23, Guanzhuang, 20180301133201	GJ, 648, 24, Zhoujiaojing, 20180301135807	



(a) Week 1

(b) Week 2

**Figure 3.** Cumulative frequency by travel counts for two weeks.

**Table 9.** An example of a high-frequency passenger network for the first week.

Travel Counts	Passengers ID	Travel Chain 1	Travel Chain 2
55	78aa216c934e339e650f119ced999979	DT, 1, 24, SiHui, 20180301065200	DT, Batong Line, 11, Liyuan, 20180301072757
55	78aa216c934e339e650f119ced999979	DT, 1, 24, SiHui, 20180301082500	DT, Batong Line, 9, Guoyuan, 20180301084903
55	78aa216c934e339e650f119ced999979	DT, 6, 53, Qingnianlu, 20180301094300	DT, 6, 57, Huangqu, 20180301095108
55	78aa216c934e339e650f119ced999979	GJ, 675, 12, Dougezhuanglu, 20180301103001	GJ, 675, 17, Qingnianlu Kou, 20180301103911
55	78aa216c934e339e650f119ced999979	DT, 6, 51, Shilibu, 20180301120000	DT, 6, 69, Beiyunhe West, 20180301123014

**Table 10.** An example of low-frequency passenger network for the first week.

Travel Counts	Passengers ID	Travel Chain 1	Travel Chain 2
10	000006c371ae0dd0336028a5149226f	DT, 2, 0, 14, East Gate, 20180301185100	DT, 6, 0, 69, Beiyunhe West, 20180301195324
10	000006c371ae0dd0336028a5149226f	DT, 6, 0, 75, Dongxiaqu, 20180304074800	DT, 2, 0, 14, East Gate, 20180304085100
10	000006c371ae0dd0336028a5149226f	DT, 2, 0, 14, East Gate, 20180304193100	DT, 6, 0, 69, Beiyunhe West, 20180304020242
10	000006c371ae0dd0336028a5149226f	GJ, 809, 1, 3, Small Arts East Area, 20180305123401	GJ, 809, 1, 19, Yunhe Mingzhujiaqu, 20180305130025
10	000006c371ae0dd0336028a5149226f	DT, 2, 0, 14, East Gate, 20180305190100	DT, 6, 0, 69, Beiyunhe West, 20180305195309

In the constructed networks, the first week data show that high-frequency passengers had a total of 3,607,960 records, while low-frequency passengers accounted for 9,538,509 records. In the second week, the high-frequency network contained 3,481,020 records, and the low-frequency network had 840,793 records. These comprehensive datasets provide a foundation for analyzing passenger travel behavior and lay the groundwork for further exploration of complex network characteristics.

#### 4.2. Complex Network Construction

In public transport systems, complex networks serve as a powerful tool for studying passenger flows, the connections between stations, and the overall efficiency and robustness of the transport system. In the construction of a complex network for public transport, this study treats stations as nodes, while the travel paths of passengers form the edges connecting these nodes.

The role of the complex network in this study is twofold: It aids in network structure analysis and in examining travel differences between high and low-frequency passengers. By constructing a complex network with stations as nodes, this paper provides an in-depth analysis of the public transportation system's structural characteristics, including the importance of stations (as measured by node degree or intermediary centrality), community structure (based on modularity optimization), and the overall connectivity of the network.

These analyses are critical for identifying key nodes and weak links within the network, offering a scientific foundation for public transport planning and optimization. Furthermore, the construction of complex networks allows for the exploration of travel behavior differences between high and low-frequency passengers at a macroscopic level. By comparing various network types within the high and low-frequency passenger networks, this study aims to reveal differences in spatial distribution and temporal usage patterns between these two groups.

In this study, the researchers take a series of steps to construct complex networks, with the primary objective of analyzing the travel differences between high and low-frequency passengers within the public transportation system, as illustrated in Figure 4.

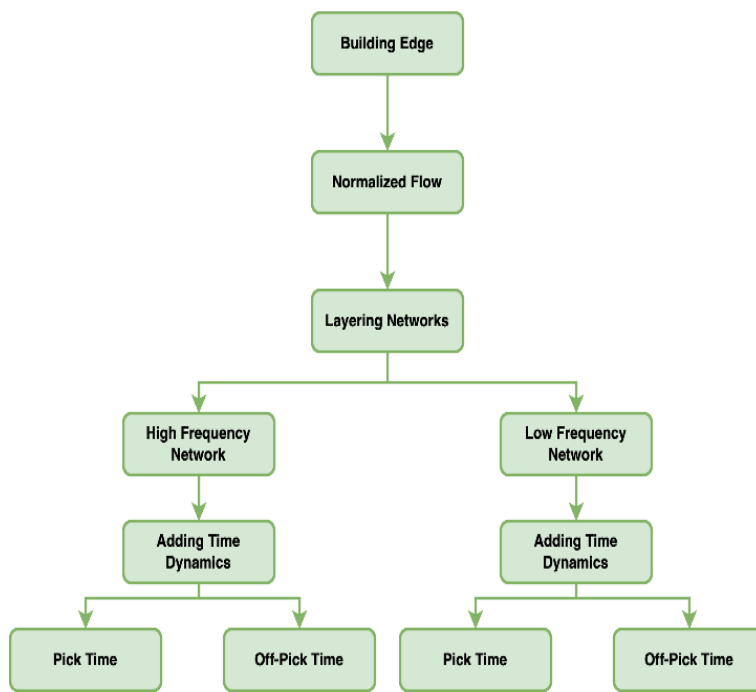


**Figure 4.** Complex construction network.

**Step 1—Node Identification:** All bus and subway stations are treated as nodes within the network. To ensure the accuracy and effectiveness of the network analysis, each station is assigned a unique identifier. In this study, the station names themselves are used directly as identifiers for the nodes.

**Step 2—Edge Construction:** Edges between nodes represent observed passenger flows between pairs of stations. For any two stations with recorded trips, a directed edge is created. The weight of each edge corresponds to the total number of passenger trips between the two stations during the analysis period, thereby reflecting the intensity of passenger movement.

**Step 3—Normalization of Flow:** Given the varying numbers of passengers in the high and low-frequency networks, max–min normalization is applied to ensure the comparability of station-to-station flow across networks. This technique scales all flow values to a unified range between 0 and 1, preserving the relative position of each value within the maximum and minimum flow values. The specific method for this normalization is presented in Formula (1).

$$\text{Normalized Flow} = \frac{\text{Flow} - \text{Min Flow}}{\text{Max Flow} - \text{Min Flow}} \quad (1)$$

This step eliminates discrepancies caused by differing passenger numbers in the high and low-frequency networks, enabling a fair comparison of flow differences across networks of different scales. It allows for a focus on the network structure itself, such as the distribution patterns of flow, the identification of key connecting stations, and the overall efficiency and robustness of the network. In the first week, the maximum observed flow was between Si Hui Hub Station and itself, with a value of 37,180, while the minimum non-zero flow was between Yanxi Station and Hongyan Station, with a value of 2. The results of the normalized edges and inter-station flows are shown in Tables 11 and 12.

**Step 4—Network Hierarchization:** The network is subdivided into two sub-networks based on the travel frequency of passengers: high-frequency and low-frequency. This division allows for a more precise analysis and comparison of the travel patterns of dif-

ferent passenger groups, revealing their impact on the structure and fluidity of the public transportation network.

**Step 5—Temporal Dynamics:** To account for passenger flow during different time periods, such as peak morning and evening hours or off-peak times, multiple network layers are created to reflect the changing travel demand over time. This temporal dimension allows the network to not only illustrate spatial passenger flow patterns but also capture the effects of temporal variations on these patterns.

**Table 11.** Normalized flow in the high-frequency passenger network for the first week.

Original Station	Destination	Flows	Normalized Flow
Si Hui Hub Station	Si Hui Hub Station	16,722	0.449743
Si Hui	Si Hui Hub Station	11,497	0.309207
Da Bei Yao South	Guomao	7641	0.205492
Si Hui Hub Station	Si Hui	6852	0.184271
Ba Wang Fen West	Da Wang Road	5846	0.157212
Si Hui Hub Station	Tongzhou Beiyuan Road East	5821	0.15654
Guomao	Da Bei Yao South	5600	0.150596
Kangjia Gou	Kangjia Gou	5431	0.14605
Da Bei Yao South	Da Bei Yao South	5157	0.13868
Qingnian Road	Qingnian Road North	4938	0.13279

**Table 12.** Normalized flow in the low-frequency passenger network for the first week.

Original Station	Destination	Flows	Normalized Flow
Si Hui Hub Station	Si Hui Hub Station	37,180	1
Si Hui	Si Hui Hub Station	24,100	0.6481885
Da Bei Yao South	Guomao	21,623	0.5815649
Da Bei Yao South	Da Bei Yao South	20,050	0.539256
Hongmiao Road East	Hongmiao Road East	18,694	0.5027838
Langjia Yuan	Guomao	16,310	0.4386616
Da Wang Road	Ba Wang Fen East	16,225	0.4363754
Kangjia Gou	Kangjia Gou	15,990	0.4300546
Guomao	Langjia Yuan	15,538	0.4178972
Guomao	Da Bei Yao South	14,112	0.3795422

#### 4.3. Visualization of Complex Networks

##### 4.3.1. Spatial Pattern Visualization

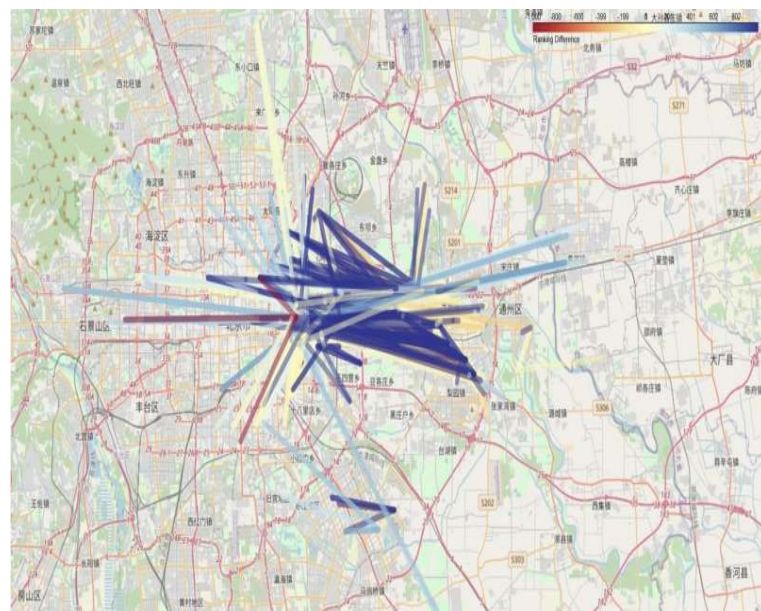
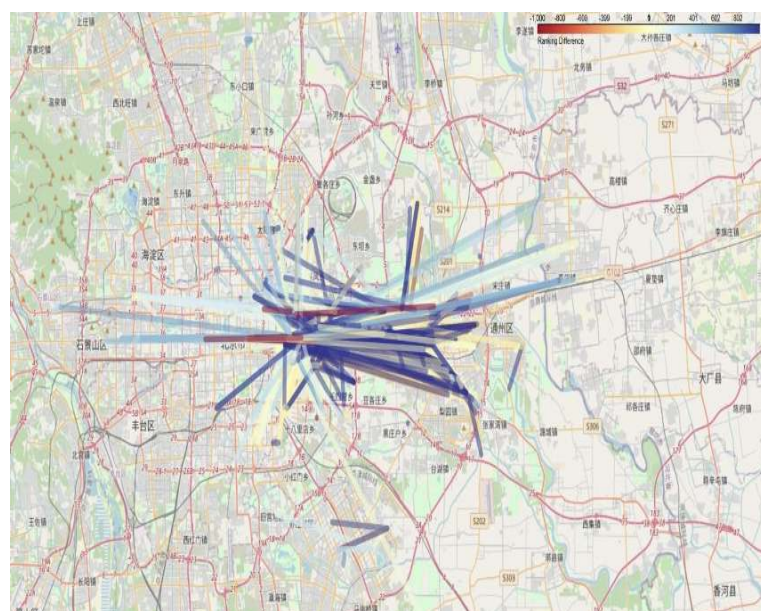
To gain a deeper understanding of the travel preferences of high- and low-frequency passengers and their impact on the transportation network, the top 1000 OD (origin-destination) pairs for each passenger group were ranked and compared. The rankings for these OD pairs were calculated separately for high-frequency and low-frequency passenger networks during peak and off-peak periods. Subsequently, the ranking differences were determined by subtracting the low-frequency ranking from the high-frequency ranking. For example, if a route ranks first in the high-frequency network but 1000th in the low-frequency network, the difference is  $-999$ . If an OD pair is absent in the low-frequency network, its ranking difference is assigned a value of  $-1000$ .

This approach provides a detailed perspective on how certain routes are predominantly used by specific user groups and are less significant for others. These differences can be attributed to passenger travel purposes or habits. For instance, high-frequency passengers might favor efficient or convenient routes for commuting, while low-frequency passengers may rely on different routes for occasional or leisure travel.

To visualize Table 13, the flow of OD pairs is displayed in different colors according to the ranking difference, corresponding to the upper right legend of Figures 5 and 6. Given the density and complexity of the spatial information in these figures, an interactive map version has been developed to facilitate detailed exploration: <https://github.com/lilieason/Transit-Network-Visual/tree/lilieason-patch-flowchart> (accessed on 3 August 2025).

**Table 13.** OD pairs of high- and low-frequency networks in the first week.

Starting Station	Terminating Station	Rank Difference
Baliqiao	Tongzhou Yangzhuang North	1000
Jishuitan	Deshengmen West	811
Dongzhimen	Zuojiazhuang	704
Beijing South Station	Da Wang Road	664
Xingda Square Community	Ba Wang Fen West	640
Dongzhimen Hub Station	Dongzhimen	628
Shuangjing Bridge North	Da Bei Yao South	623
Zhongzhaofu Village	Langjia Yuan	614
Langjia Yuan	Xingda Square Community	614
Guomao	Wukesong	613

**Figure 5.** Passenger flow chart for high-frequency and low-frequency users in the first week.  
Note: Chinese labels in the map indicate actual station names in Beijing's transit system.**Figure 6.** Passenger flow chart for high-frequency and low-frequency users in the second week.  
Note: Chinese labels in the map indicate actual station names in Beijing's transit system.

#### 4.3.2. Temporal Flow Visualization

In this study, as illustrated in Table 14, the travel records of each passenger are marked by identifying their initial card-swiping event as the starting point to construct their travel chain dataset for specific time slots. For example, the passenger with the ID “78aa216c934e339e650f119ced699979” performed their first card swipe at several distinct times on 1 March 2018, each corresponding to a different travel chain. The initial card-swiping event serves as a precise timestamp for each travel chain, enabling the systematic compilation of all passengers’ first card-swiping events within each defined time slot.

**Table 14.** Example of passenger travel chains.

Travel Instances	Passenger ID	Travel Chain 1
55	78aa216c934e339e650f	DT, 1, 24, Si Hui, 20180301065200
55	78aa216c934e339e650f	DT, 1, 24, Si Hui, 20180301082500
55	78aa216c934e339e650f	DT, 6, 53, Qingnian Road, 20180301094300
55	78aa216c934e339e650f	GJ, 675, 12, Dougezhuang South, 20180301103001
55	78aa216c934e339e650f	DT, 6, 51, Shilbao, 20180301120000
55	78aa216c934e339e650f	DT, 1, 24, Si Hui, 20180301065200
55	78aa216c934e339e650f	DT, 1, 24, Si Hui, 20180301082500

This compilation forms a robust dataset that captures the flow of passengers during specific time periods. Such data provides the foundation for further analysis, enabling a detailed examination of travel patterns and identifying peak period flows. This approach is essential for understanding temporal dynamics in the public transportation system and offers valuable insights for optimizing service schedules and resource allocation.

The described method allows for recording the total number of card swipes within each time slot, providing a detailed view of passenger activity during specific periods. By further aggregating the number of swipes across all days of the week for each time slot, the total passenger flow for each time slot throughout the entire week can be determined. This aggregation provides a comprehensive dataset for analyzing weekly travel patterns and identifying peak usage periods. The summarized results are presented in Table 15.

**Table 15.** Total passenger flow for each time slot throughout the week.

Time Slot	High-Frequency Week 1	Low-Frequency Week 1	High-Frequency Week 2	Low-Frequency Week 2
00-02	873	1689	923	1508
02-04	481	994	541	797
04-06	31,984	75,706	45,361	71,866
06-08	574,449	1,128,045	577,760	1,021,976
08-10	685,076	1,538,264	642,371	1,428,009
10-12	255,185	792,695	251,382	784,971
12-14	260,506	819,192	262,857	839,557
14-16	265,715	878,660	267,877	870,069
16-18	492,632	1,328,076	485,278	1,213,996
18-20	661,251	1,313,580	605,854	1,165,313
20-22	305,452	544,129	273,537	529,395
22-24	74,355	117,478	67,278	113,334

As illustrated in Figure 7 the passenger flow distribution reveals two distinct peaks in the daily travel cycle: the morning peak (06:00–08:00) and the evening peak (18:00–20:00). During these periods, passenger flow increases significantly, highlighting the concentrated travel demand. This periodic fluctuation provides a clear basis for defining the morning and evening peak periods.

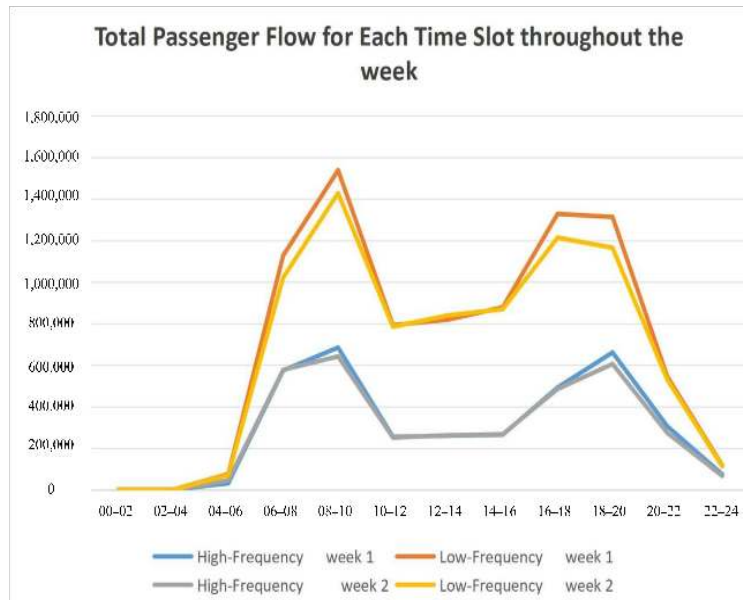


**Figure 7.** Total passenger flow for each time slot throughout the week.

Given the differences in the size of high- and low-frequency passenger groups, it is essential to standardize the passenger flow data to ensure accurate comparisons. The standardized data, presented in Table 16, reflects the distribution characteristics of passenger flow in the two networks more effectively, enabling a detailed examination of travel behaviors and patterns between high- and low-frequency passenger groups. This standardized approach allows for a clearer understanding of the unique dynamics within each network.

**Table 16.** Normalized passenger flow for each time slot throughout the week.

Time Interval	Normalized High-Frequency Week 1	Normalized Low-Frequency Week 1	Normalized High-Frequency Week 2	Normalized Low-Frequency Week 2
00-02	0.000254912	0.000785546	0.000287427	0.000667845
02-04	0	0.000333597	0.0000390172	0.000205491
04-06	0.020485985	0.048917825	0.029184872	0.046420724
06-08	0.373243819	0.733239996	0.375396919	0.664264724
08-10	0.445183098	1.000000000	0.417412600	0.928302628
10-12	0.165630651	0.515166314	0.163157611	0.510143499
12-14	0.169090828	0.532396964	0.170619652	0.545640055
14-16	0.172478171	0.571068220	0.173884092	0.565481606
16-18	0.320039303	0.863317516	0.315257094	0.789132797
18-20	0.429690015	0.853890959	0.393666076	0.757474884
20-22	0.198318618	0.353527123	0.177564715	0.343945797
22-24	0.048039288	0.076081606	0.043437208	0.073386817

Analyzing Figure 8 yields several important insights into the travel behaviors of high- and low-frequency passengers:

(1) Figure 8 highlights that the orange and yellow curves, representing low-frequency passengers, consistently show a higher flow ratio compared to the high-frequency passenger curves, indicated by the blue and gray lines. This pattern correlates with the overall distribution of passenger numbers, where low-frequency passengers outnumber high-frequency passengers by approximately three to one. However, the flow ratio for low-frequency passengers is only about twice as much, suggesting a relatively higher usage intensity by high-frequency passengers.

(2) Across different times of the day, the travel trends of high- and low-frequency passengers exhibit similar patterns, particularly during the morning peak (8:00–10:00) and evening peak (18:00–20:00), where both groups reach maximum flow levels. However,

a significant divergence is observed during the evening peak period, where the flow of low-frequency passengers stabilizes or slightly declines, while high-frequency passenger flow increases. This distinction may reflect the specific activities or work routines of high-frequency passengers, such as extended work hours or evening commutes.

(3) Over the course of the day, the flow difference between high- and low-frequency passengers gradually widens, peaking during the morning and evening rush hours (8:00–10:00). This widening gap could indicate a higher dependency on public transportation among high-frequency passengers during these critical periods. However, during nighttime hours, the flow difference between the two groups becomes almost negligible, suggesting that under conditions of lower overall travel demand, travel frequency plays a less significant role in shaping flow patterns. This observation underscores the importance of optimizing nighttime public transportation services, with a focus on addressing the specific travel needs of both passenger groups.

These findings provide a nuanced understanding of passenger behavior and can guide transportation planners in optimizing services for different passenger segments, particularly during peak and off-peak periods.

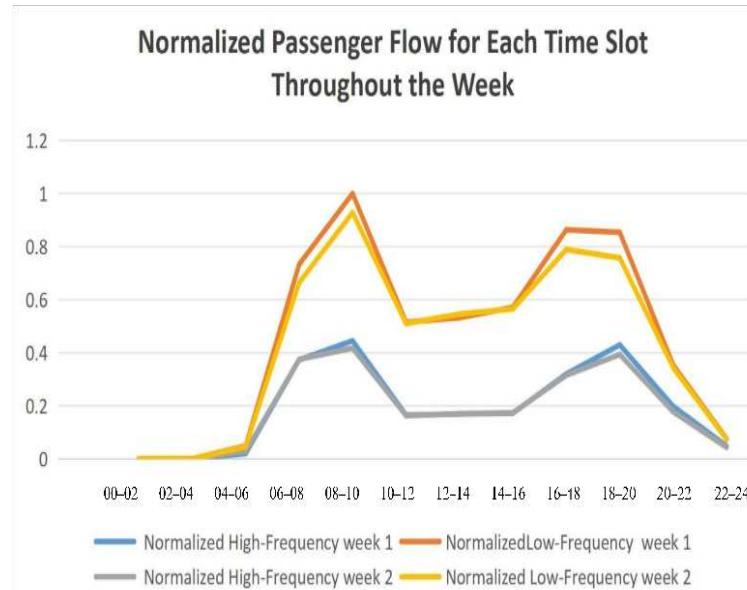


**Figure 8.** Standardized passenger flow for each time.

#### 4.3.3. Integrated Spatiotemporal Visualization

Following the time analysis in the previous section, it is evident that the travel peaks occur between 8:00–10:00 AM and 18:00–20:00 PM. Based on these peak times, this section provides a spatiotemporal visual analysis of the station flow during these periods. The station flow data for the morning and evening peaks are shown in Tables 17 and 18.

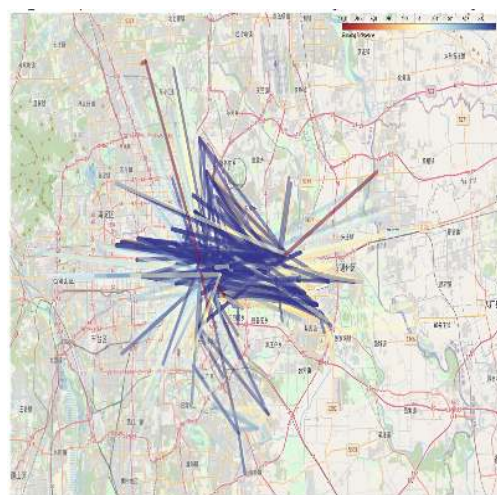
Approximately 130,000 data points from the morning and evening peaks of the high-frequency passenger network and around 190,000 inter-station traffic data points from the low-frequency network during the same periods were collected. Using the same visualization approach outlined in Section 3.3, maps depicting the morning and evening peak hours for both high- and low-frequency passenger networks were created. The visualization focuses on the 1000 busiest routes, with line color contrasts and thickness emphasizing the frequency of travel. These results are illustrated in Figures 9 and 10. To enhance clarity and support detailed examination, interactive versions of these visualizations have been made available at: <https://github.com/lilieason/Transit-Network-Visual/tree/lilieason-patch-peakhour> (accessed on 3 August 2025).

**Table 17.** High-frequency passenger flow between the morning rush-hour stations in the first week.

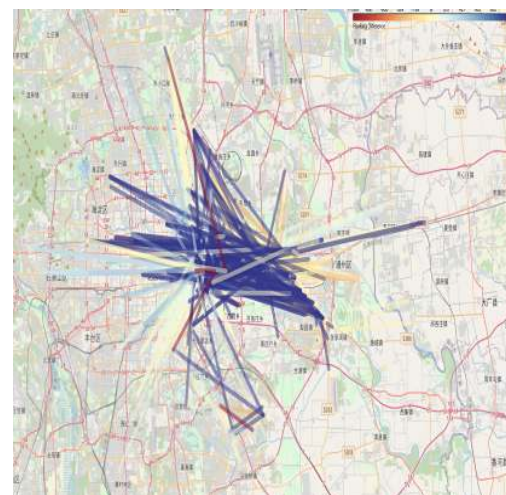
Starting Station	Terminating Station	Flow
Da Bei Yao South	Guomao	4962
Ba Wang Fen West	Da Wang Road	3581
Si Hui Hub Station	Si Hui	3125
Tuqiao Village	Tuqiao	3066
Si Hui East Station	Si Hui East	2493

**Table 18.** High-frequency passenger flow between the evening rush-hour stations in the first week.

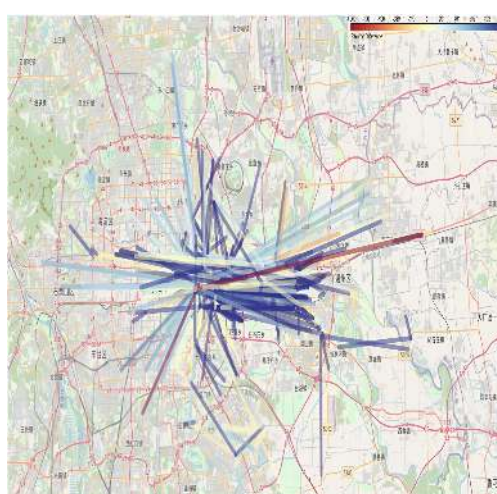
Starting Station	Terminating Station	Flow
Si Hui	Si Hui Hub Station	4456
Guomao	Da Bei Yao South	2918
Si Hui Hub Station	Tongzhou Beiyuan Road East	2729
Guan Zhuang	Yangzha Road South	2417
Guomao	Langjia Yuan	1983



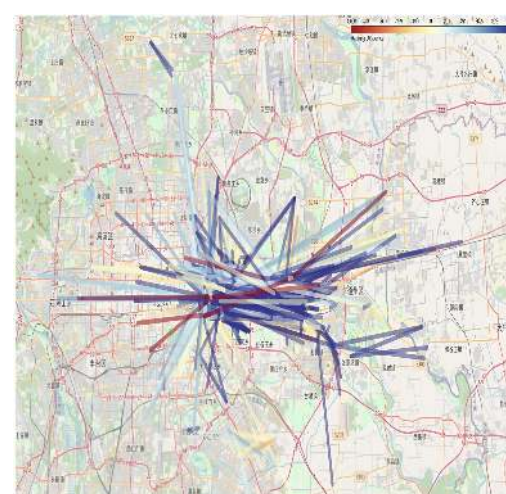
(a) Week 1 HF Network Morning Peak



(b) Week 1 HF Network Evening Peak

**Figure 9.** Comparison of morning peak (a) and evening peak (b) for high-frequency network in week 1. Note: Chinese labels in the maps indicate actual station names in Beijing's transit system.

(a) Week 1 LF Network Morning Peak



(b) Week 1 LF Network Evening Peak

**Figure 10.** Comparison of morning peak (a) and evening peak (b) for low-frequency network in week 1. Note: Chinese labels in the maps indicate actual station names in Beijing's transit system.

#### 4.3.4. Cluster Visualization

This study constructs a daily travel chain network for bus passengers, representing stations as nodes and passenger travel chains as edges. Using a unified storage format, the structured database allows easy retrieval of travel trajectories and detailed analysis of the spatial and temporal characteristics of bus trips.

High- and low-frequency passenger networks are also developed by distinguishing station usage frequencies. The high-frequency network highlights frequently used connections, while the low-frequency network captures less utilized links. This approach enables a detailed exploration of travel behavior and supports the precise optimization of the bus network.

Visualization extends beyond graphical representation, incorporating analysis to reveal differences between high- and low-frequency networks. By comparing standardized flow maps across time periods, peaks, valleys, and distinct activity patterns of passenger groups are observed, offering insights for better network planning, as shown in Figures 11 and 12. To support more detailed exploration of these temporal and spatial dynamics, interactive heatmap visualizations are available at: <https://github.com/lilieason/Transit-Network-Visual/tree/lilieason-patch-heatingmap> (accessed on 3 August 2025).

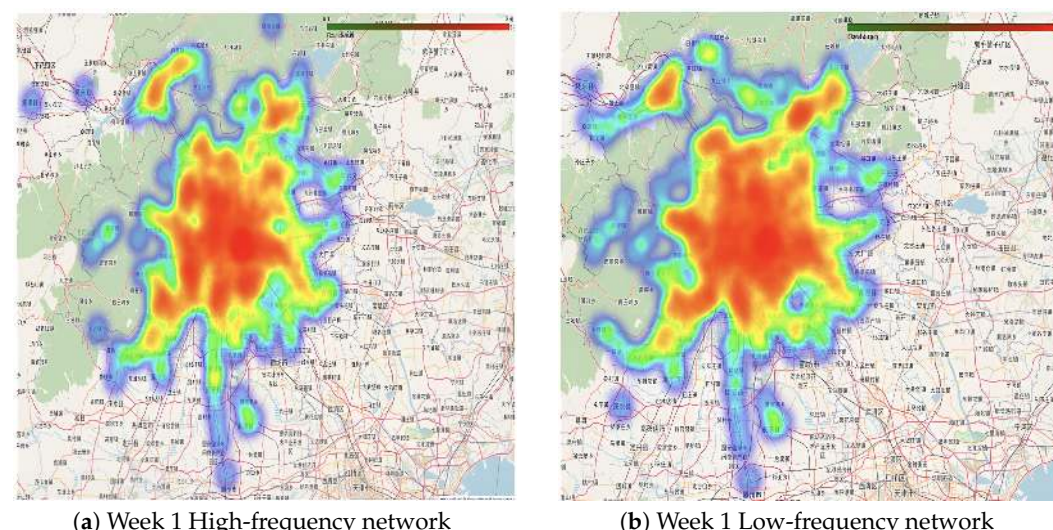


**Figure 11.** High-frequency (a) and low-frequency (b) passenger networks in week 1. Note: Chinese labels in the maps indicate actual station names in Beijing's transit system.

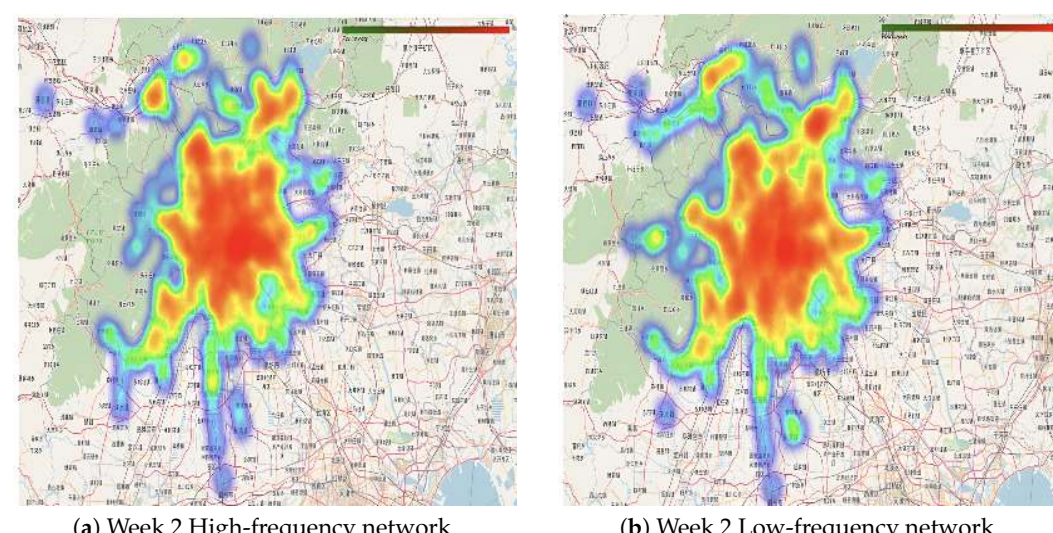


**Figure 12.** High-frequency (a) and low-frequency (b) passenger networks in week 2. Note: Chinese labels in the maps indicate actual station names in Beijing's transit system.

## 5. Complex Network Characteristics Analysis

### 5.1. Node Analysis

A comprehensive analysis of node degree, Betweenness centrality, and closeness centrality provides a deep understanding of the structural characteristics and operational status of the transportation network. This approach helps identify key nodes, referred to as central stations, which are marked by high node degree, high Betweenness centrality, and high closeness centrality. These central nodes hold strategic significance within the network, serving as critical hubs for connectivity and flow management.

The node degree correlation indices of the network are presented in Table 19. In each box plot, the bottom and top of the box represent the first quartile (Q1) and the third quartile (Q3), respectively, while the line within the box indicates the median. Points outside the box extend to the minimum and maximum of the data distribution or are located beyond 1.5 times the interquartile range, which are considered potential outliers and may represent special cases or anomalies.

**Table 19.** Example of the centrality index of the high-frequency network nodes in the first week.

Node	Node Degree	Betweenness Centrality	Closeness Centrality
234	584	0.032328503	0.72360253
121	576	0.02718349	0.720026241
431	519	0.017041975	0.686116057
245	516	0.021768721	0.677606091
470	505	0.012482327	0.672393736
42	492	0.013863119	0.662205952
292	487	0.022916277	0.670331179
392	486	0.021179668	0.669304638
154	478	0.012861307	0.647490264
357	467	0.011550909	0.656240133

An average line, depicted in red, is included to provide an additional measure of central tendency. To evaluate whether statistically significant differences exist among the same index groups across different network states, the Mann-Whitney U test is conducted. The *p*-value results from this test are used to determine whether the “no difference” hypothesis can be rejected, with a *p*-value less than 0.05 indicating significant differences.

When comparing the node degree distribution of the high-frequency passenger complex network over two time periods, the results reveal significant statistical differences. The *p*-value for group 01 is 0.022, and the *p*-value for group 02 is 0.033, both of which are below the traditional significance threshold of 0.05. This indicates that there are statistically significant differences in the node degree distribution between the high-frequency and low-frequency networks across the two periods.

As shown in Figure 13, the median node degree is generally lower in the high-frequency network than in the low-frequency network. This finding suggests that the sites in low-frequency networks are typically connected to a larger number of other sites, forming a more active network of traffic nodes. This characteristic reflects the central role of certain stations in the low-frequency network, such as major transportation hubs or commercial centers, which exhibit higher node degrees due to serving a larger volume of passengers or connecting more lines.

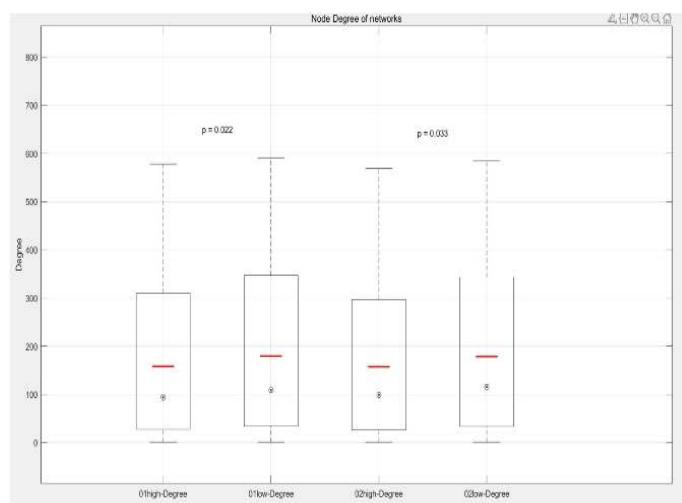


**Figure 13.** Box plots of node degree.

In contrast, the lower median node degree in high-frequency networks may indicate that the stations primarily used by high-frequency passengers tend to occupy more peripheral or marginal positions in the overall station network. This distinction underscores the differing roles and spatial characteristics of stations in high- and low-frequency passenger networks.

When comparing the betweenness centrality distribution of high-frequency and low-frequency passenger networks across the two periods, the observed *p*-values are 0.708 and 0.929, respectively. Since these values are significantly above the standard significance threshold of 0.05, it can be concluded that there is no statistically significant difference in Betweenness centrality between the two networks. This indicates that the importance of stations as passenger traffic transfer points remains relatively consistent in both high-frequency and low-frequency networks.

As shown in Figure 14, the medians of all groups are similar, and while outliers are present, they do not influence the overall comparison between the groups. These outliers likely correspond to specific stations with particularly significant or unusual transit roles within the network. Although the Betweenness centrality of such stations may be critical to their respective networks, their influence does not result in significant differences in the overall distribution of Betweenness centrality.

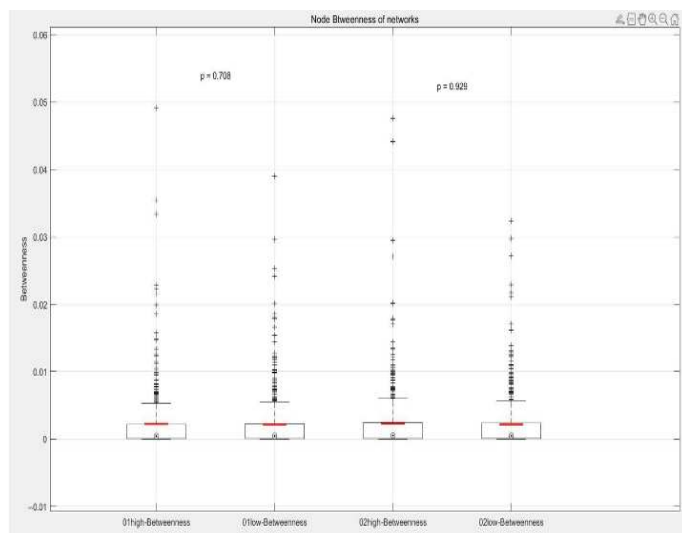


**Figure 14.** Box plots of betweenness centrality.

This analysis suggests that while certain stations may have unique transit roles during specific periods, these roles do not create substantial distinctions between high- and low-frequency networks from a network-wide perspective. This consistency implies that the transit functions and network structure of the stations remain stable, even under varying passenger flows. Furthermore, it highlights the robustness of the network design, where stations can effectively maintain their connection and transfer functions regardless of fluctuations in passenger activity.

As shown in Figure 15, groups 01 and 02 demonstrate a statistically significant difference in closeness centrality. The  $p$ -value for group 01 is 0.015, and for group 02 it is 0.035, both of which are below the conventional significance threshold of 0.05. This indicates substantial differences in the closeness centrality of nodes between the two time periods.

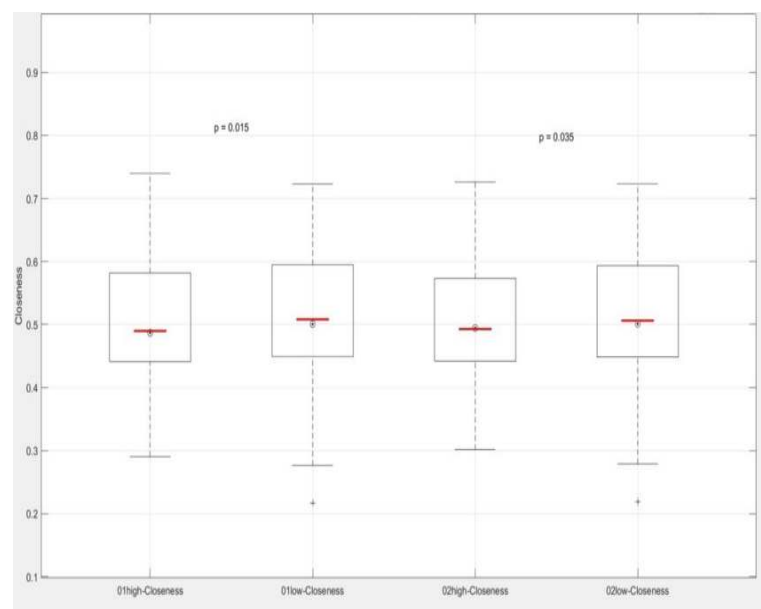


**Figure 15.** Box plots of closeness centrality.

Analysis of these differences reveals that the closeness centrality of sites in the low-frequency network is generally higher compared to the high-frequency network. This likely reflects the strategic positioning of sites within the low-frequency network, enabling passengers to reach other stations more quickly. However, given the smaller number of high-frequency passengers, the difference in closeness centrality between the two networks is not pronounced. This suggests that stations in the high-frequency network also provide efficient connectivity, particularly for frequent travelers, such as commuters, who may prioritize time savings and rely on these stations.

Additionally, the upper and lower bounds of closeness centrality in the high-frequency network are higher than those in the low-frequency network. This finding indicates that it is easier to reach other stations within the high-frequency network, further emphasizing its efficiency in catering to passengers with frequent travel needs.

In the low-frequency network, the lower limit of closeness centrality is lower, while the average and median are higher. This suggests that the low-frequency network includes stations located in more remote areas or slightly away from the main routes of the urban transportation network.

Comprehensive analysis of the three node indicators reveals key insights. The significant differences in node degree indicate that some stations bear higher traffic in the low-frequency network, playing a critical role in passengers' daily travel. Conversely, in the high-frequency network, traffic is more evenly distributed across stations, with passenger

flow less concentrated at specific sites. Although the geographical positions of stations remain constant, their importance within the network shifts with passenger traffic patterns.

The analysis of Betweenness centrality shows that the strategic role of stations as passenger flow transit points remains consistent between high- and low-frequency networks. This consistency suggests that, despite variations in overall traffic volume, passenger flow paths and routes between stations are relatively stable.

Differences in closeness centrality highlight the higher accessibility of sites in the high-frequency network, reflecting improved connectivity and efficiency under conditions of high passenger traffic. This allows passengers, particularly frequent travelers, to reach destinations more quickly.

For improving the high-frequency network, given the smaller number of passengers but higher closeness centrality at some nodes, priority should be given to increasing the transportation capacity at these central stations or enhancing their transfer efficiency. Additionally, to address the concentration of high-degree nodes, constructing new routes or increasing the capacity of existing ones could help distribute traffic more evenly and enhance the network's overall robustness and capacity.

In the low-frequency network, for nodes with lower traffic, increasing direct connections to high-demand nodes could improve their accessibility and appeal. This would enhance the utilization and efficiency of these underused parts of the network, contributing to a more balanced and effective transportation system.

## 5.2. Robustness Test

According to the summary of the indicators in the above section, the top 10 nodes with the highest comprehensive scores in the network are selected as the central nodes. The comprehensive score is calculated by summing the Z-score normalized values of node degree, Betweenness centrality, and closeness centrality for each node. This selection criteria ensures a holistic evaluation of the nodes' performance across these three metrics, identifying the most prominent and strategically significant nodes in the network.

The Z-score (Z value) is a standard statistic used to measure the deviation of a data point from the sample mean, expressed in units of the sample standard deviation. Z-score normalization ensures that all indicators are on the same scale, allowing for a fair comparison and aggregation of metrics. The formula for the Z-score is:

$$Z = \frac{(X - \mu)}{\sigma} \quad (2)$$

where  $X$  represents the value of the original data point,  $\mu$  is the mean of the sample, and  $\sigma$  is the standard deviation of the sample. The Z-score calculations standardize the data, eliminating dimensional differences between variables. This standardization facilitates comparisons and enables a comprehensive assessment of the variables, ensuring each metric contributes equally to the overall score.

Using this method, the central nodes of the network were identified, and the results are summarized in Table 20. This table highlights the nodes with the highest comprehensive scores, reflecting their significant roles within the network based on their node degree, betweenness centrality, and closeness centrality.

To explore the robustness of high-frequency and low-frequency passenger traffic networks, this study employs four key indicators: global clustering coefficient, strongly connected components, average path length, and network efficiency. Leveraging optimization techniques, including neural network-based modeling for decision-making, maintenance strategies in networked systems, and adaptive learning algorithms for decentralized architectures, has been shown to enhance network resilience and efficiency [35–37]. By

identifying central nodes, as described before, a comparative analysis is conducted by examining the changes in these indicators before and after the removal of central nodes. This approach reveals the robustness of high- and low-frequency passenger complex networks when critical nodes fail, providing insights into the networks' ability to maintain connectivity and functionality under such disruptions. Tables 21 and 22 present the network features before and after the removal of central sites.

**Table 20.** Center nodes of the high- and low-frequency network.

Network	01high	01low	02high	02low
Central_Node_1	234	234	121	234
Central_Node_2	121	121	234	121
Central_Node_3	245	470	431	494
Central_Node_4	431	494	470	292
Central_Node_5	470	245	42	245
Central_Node_6	292	392	245	392
Central_Node_7	392	431	402	431
Central_Node_8	154	292	392	42
Central_Node_9	42	42	292	470
Central_Node_10	402	357	511	154

**Table 21.** Network features before the removal of central sites.

Complex Network	Global Agglomeration Coefficient	Strong Connectivity Component	Average Path Length	Network Efficiency
01high	0.000963703	18	$2.00754 \times 10^{-6}$	40,195.4662
02high	0.000737876	14	$1.01798 \times 10^{-6}$	45,516.9691
01low	0.000941457	13	$1.41143 \times 10^{-6}$	38,284.88213
02low	0.000958783	15	$1.57739 \times 10^{-6}$	41,033.7702

**Table 22.** Network features after the removal of central sites.

Complex Network	Global Agglomeration Coefficient	Strong Connectivity Component	Average Path Length	Network Efficiency
01high	0.001157316	18	$1.7097 \times 10^{-6}$	38,952.73212
02high	0.000778501	14	$9.1119 \times 10^{-7}$	43,540.0276
01low	0.000870484	11	$8.81033 \times 10^{-7}$	46,680.90104
02low	0.00089554	12	$1.36916 \times 10^{-6}$	40,090.89339

For the high-frequency networks, a slight decrease in the global clustering coefficient was observed after the removal of central nodes. For instance, in the first week, the clustering coefficient dropped from 0.001157316 to 0.000963703. This change indicates that the overall network structure remained relatively stable, though the removal of central nodes slightly affected local connectivity. However, network efficiency showed a significant decrease in both high-frequency networks, underscoring the importance of central nodes in maintaining overall communication efficiency.

Low-frequency networks exhibited different robustness characteristics. Interestingly, the clustering coefficient increased slightly after the removal of central nodes, such as in the 01low network, where it rose from 0.000870484 to 0.000941457. This may reflect better connectivity in other parts of the network or the presence of more alternative paths in low-frequency networks. Nonetheless, similar to high-frequency networks, the average path length in low-frequency networks increased, and network efficiency decreased, emphasizing that central nodes are also critical for the performance of low-frequency networks.

Overall, both high- and low-frequency networks showed structural changes after the removal of central nodes. The decline in the clustering coefficient and the significant reduction in network efficiency for high-frequency networks highlight their dependency on central nodes. The efficiency drop of 5% and the clustering coefficient reduction of 0.1% may be attributed to the concentrated traffic flow and limited route diversity in high-frequency passenger movements. Conversely, the increased clustering coefficient in low-frequency networks suggests that other parts of the network retain structural integrity, even with central node removal. However, the increase in average path length and the decrease in network efficiency across both network types reinforce the critical role of central nodes in ensuring efficient network operation.

### 5.3. Basic Property Analysis of Complex Networks

#### 5.3.1. Cluster Coefficient

The agglomeration coefficient measures the extent to which a site's adjacent nodes are interconnected. Specifically, it represents the likelihood that if a site A has direct connections with both sites B and C, there is also a direct connection between B and C. This metric reflects the clustering tendency in the network, capturing the local tightness and formation of small group structures.

The global agglomeration coefficient, in contrast, measures the actual proportion of all possible triangular relationships across the entire network. It provides an overall assessment of the network's clustering tendency, extending the concept of the local agglomeration coefficient to the entire system. This metric reveals how closely nodes are interconnected on a network-wide scale.

In this study, the weighted global agglomeration coefficient is calculated using `nx.average_clustering(G, weight = 'traffic')`, which accounts for the traffic flow between nodes as a weight. High values of the global agglomeration coefficient indicate the presence of many closely connected groups of nodes, suggesting an effective network design capable of dispersing and managing high traffic efficiently.

For Table 23, the observed global agglomeration coefficients for high-frequency networks are 0.001157316 and 0.000778501, showing higher values compared to the low-frequency networks, which are 0.000870484 and 0.00089554, respectively. This suggests that high-frequency networks exhibit more closed loops and three-node connections among their nodes. The characteristics of this network structure may be influenced by the daily commuting behavior of high-frequency passengers, who tend to utilize various routes to meet their diverse travel needs.

**Table 23.** Global agglomeration coefficient of each network.

Complex Networks	Global Agglomeration Coefficient
01high	0.001157316
02high	0.000778501
01low	0.000870484
02low	0.00089554

In contrast, the low-frequency networks display lower and relatively consistent agglomeration coefficients, indicating fewer direct connections between nodes. This simpler and more concentrated network structure likely reflects a tendency among low-frequency passengers to use major traffic routes or direct paths to reach primary destinations, rather than relying on complex networks requiring multipath selections as seen with high-frequency passengers.

The higher agglomeration coefficient observed in high-frequency networks highlights their complex and highly interconnected structure. This complexity is likely due to daily

commuters needing to access multiple destinations within the city, such as workplaces, schools, or shopping centers, resulting in more extensive and variable route choices. This structural difference underscores the varying network design requirements for catering to the distinct travel behaviors of high- and low-frequency passengers.

### 5.3.2. Strongly Connected Component

By analyzing strongly connected components, this study identifies potential weak links or performance bottlenecks, enabling the proposal of improvement measures to optimize network design, enhance risk management, and improve service capability.

On a technical level, the identification of strongly connected components is achieved using a graph traversal algorithm. Specifically, the number of strongly connected components in this study is determined by the `strongly_connected_components` function provided by the network analysis library. This function employs depth-first search (DFS) to systematically explore the network. Each time an unvisited node is encountered during the DFS traversal, a new strongly connected component is identified and explored. This process continues until all nodes in the graph have been fully analyzed, providing a comprehensive understanding of the network's connectivity and structural integrity.

A strongly connected component analysis of high- and low-frequency passenger traffic networks reveals variations in network connectivity across different periods and their behavioral implications. Based on the results in Table 24, several conclusions can be drawn.

**Table 24.** Strong connected component of each network.

Complex Networks	Strong Connectivity Component
01high	18
02high	14
01low	11
02low	12

The comparison of strongly connected components between high- and low-frequency networks highlights notable differences. In the first week, the high-frequency network had significantly more strongly connected components than the low-frequency network (11 vs. 7). In the second week, this difference was smaller but still present (14 vs. 12). These distinctions likely reflect differences in passenger travel behavior. High-frequency networks primarily represent the travel patterns of daily commuters, characterized by more dispersed paths and nodes in the urban transportation network. In contrast, low-frequency networks correspond to non-daily or traveler behaviors, with relatively concentrated travel paths along primary or specific routes.

The higher number of strongly connected components in the high-frequency network suggests that commuters utilize a wider range of paths and connections, contributing to a more dispersed network structure. Conversely, the smaller number of strongly connected components in the low-frequency network indicates a tendency for travelers to use concentrated and predictable routes. These findings align with previous analyses, further emphasizing the differing network dynamics driven by the behaviors of high- and low-frequency passenger groups.

### 5.4. Average Path Length

The average shortest path length represents the average “cost” of transferring information between nodes or completing a journey within a directed graph. In the context of high- and low-frequency passenger complex networks studied in this paper, this metric provides insights into the average direct accessibility of passengers within the network.

The method employed in this study calculates the average shortest path length for all node pairs within the largest strongly connected component of the directed graph. This calculation is performed using the `average_shortest_path_length` function from the NetworkX library. The process leverages the depth-first search (DFS) algorithm for weighted graphs, incorporating “normalized traffic” as edge weights. Here, the weight of each edge reflects the relative traffic flow between two sites.

By using these weights in the calculation, the shortest path length is measured based on the cumulative traffic values along the path. Consequently, the resulting average shortest path length reflects not only the spatial characteristics of the network but also the average flow efficiency of passengers within it, providing a comprehensive view of the network’s performance. The formula is expressed as follows:

$$Z = \frac{1}{|S|(|S| - 1)} \sum_{\substack{u,v \in S \\ u \neq v}} d(u, v) \quad (3)$$

where,  $|S|$  represents the number of nodes in the largest strongly connected component being analyzed, and  $d(u, v)$  denotes the shortest path length from node  $u$  to node  $v$ . The path length is calculated using the weights assigned to the edges, where the weights correspond to standardized traffic values. This means that the shortest path length is a weighted measure reflecting the relative traffic flow between nodes, rather than the actual physical distance or travel time. This approach provides a more nuanced understanding of the network’s accessibility and flow efficiency.

From the data in Table 25, the high-frequency network (01high and 02high) and the low-frequency network (01low and 02low) exhibit notable differences in average shortest path length. Specifically, the high-frequency network, particularly 01high, has a longer average shortest path length. This suggests that the travel paths of daily commuters are more complex compared to low-frequency travelers.

**Table 25.** The average shortest path of each network.

Complex Networks	Average Shortest Path
01high	$1.7097 \times 10^{-6}$
02high	$9.1119 \times 10^{-7}$
01low	$8.81033 \times 10^{-7}$
02low	$1.36916 \times 10^{-6}$

In high-frequency networks, commuters often require more transfers and links, reflecting the need to navigate between various locations such as workplaces, residences, and urban services. This complexity may arise from the larger distances between key destinations or the network’s design, which aims to offer broader coverage and more transfer options to accommodate diverse commuting needs.

However, a longer average shortest path length may also highlight potential inefficiencies in the network. For commuters, extended paths can result in increased travel time and higher costs, potentially influencing their travel behavior and even their choices of residence and workplace. This underscores the importance of optimizing network design to balance accessibility with efficiency for frequent travelers.

As observed from Table 26, the low-frequency network in the first week exhibits the highest network efficiency, indicating that travelers in this network generally experience lower “traffic costs” to reach their destinations. This aligns with the shorter average shortest path length observed in the 01low network, suggesting that low-frequency networks provide more direct and efficient travel routes for their users.

**Table 26.** Network efficiencies of each network.

Complex Networks	Network Efficiencies
01high	38,952.73212
02high	43,540.0276
01low	46,680.90104
02low	40,090.89339

In contrast, high-frequency networks, particularly in the first week, demonstrate relatively lower efficiency. This reflects the higher flow costs associated with daily commuters who often traverse multiple nodes and connections to complete their journeys. The high-frequency networks serve a broader range of areas to accommodate passengers traveling between work, educational institutions, and other urban locations, which are frequently farther apart. Consequently, while high-frequency passenger routes are more complex and involve more transfers, this complexity also highlights the transportation network's capacity to serve a diverse range of destinations.

The lower efficiency in high-frequency networks suggests potential opportunities for network optimization, especially during peak hours when commuter demand is highest. Reduced path efficiency during these times can exacerbate congestion and delays, increasing travel costs and potentially affecting commuters' travel choices and overall quality of life.

Additionally, the global agglomeration coefficient of the high-frequency network (0.0009679085) is slightly higher than that of the low-frequency network (0.0008830120), and the high-frequency network also features a greater number of strongly connected components. These characteristics indicate that the high-frequency network structure is relatively loose, with weaker site connections, while the low-frequency network exhibits a more compact structure with stronger inter-site connections. This disparity can be attributed to the more complex and diverse travel patterns in high-frequency networks, which include more sites and routes, resulting in a more intricate network topology. The increased indirect connectivity and redundant paths in high-frequency networks lead to a 16% increase in average path length and a corresponding 5% decrease in network efficiency.

The Louvain Community Detection Algorithm is a hierarchical clustering approach based on modularity optimization, designed to uncover highly modular community structures within a network. Modularity measures the quality of network segmentation, where a highly modular segmentation contains numerous internal edges (connections within a community) and fewer external edges (connections between communities).

This information allows traffic planners to allocate resources more effectively, such as enhancing transport capacity in busier communities or introducing customized services in low-frequency areas. By reducing redundant connections between communities and strengthening services within each community, transportation systems can improve efficiency, minimize congestion, and enhance passenger satisfaction. Additionally, community detection provides a foundation for planning new routes and services. Identified communities that diverge from the existing transportation network may indicate opportunities for potential new lines or services tailored to meet emerging passenger demands.

After performing visual community detection, over 500 cluster sites were grouped into multiple communities, each represented by a distinct color. The flow between communities is visualized using green lines connecting the center points of the communities, with the thickness of the lines corresponding to the flow size. Similarly, the flow within each community is depicted by the size of the circle at the community's center point. These visualizations effectively illustrate the distribution of inter-community and intra-community flows. The results of this analysis are presented in Figures 16 and 17. To facilitate a more detailed exploration of the modular structure and community interactions,

interactive versions of these community detection visualizations are available at: <https://github.com/lilieason/Transit-Network-Visual/tree/lilieason-patch-community> (accessed on 3 August 2025), and have also been included in the Appendix A.

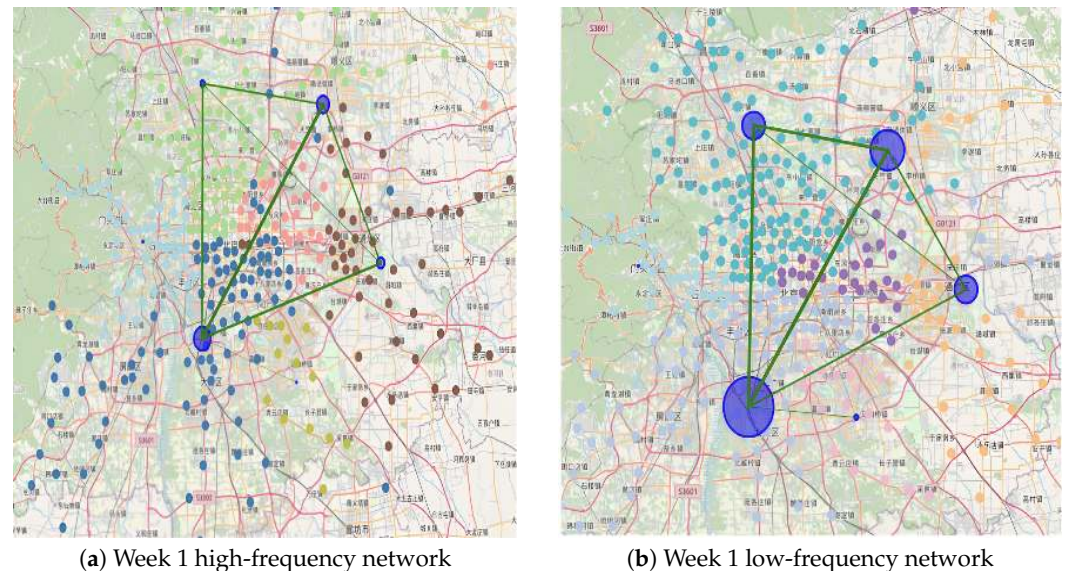


**Figure 16.** High-frequency (a) and low-frequency (b) network community detection in week 1. Note: Chinese labels in the maps indicate actual station names in Beijing's transit system.

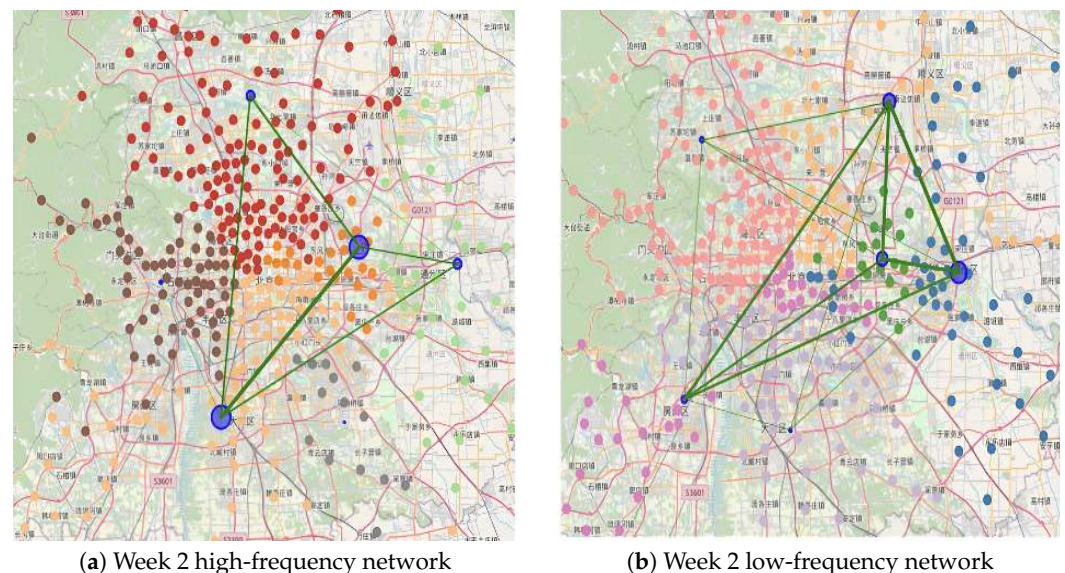


**Figure 17.** High-frequency (a) and low-frequency (b) network community detection in week 2. Note: Chinese labels in the maps indicate actual station names in Beijing's transit system.

In the visualization map of the high- and low-frequency passenger networks during the first week, the distribution and connections between central nodes appear similar. However, in the second week, the high-frequency passenger network exhibits larger communities with more stations within each community, whereas the low-frequency passenger network has a greater number of communities with more distinct divisions and closer internal connections.

To further analyze the complex networks following community detection, three indicators are used to characterize the networks. The size represents the number of nodes within a community, offering insight into the scale of individual communities. The average degree is the mean number of edges per node in the network, providing a macroscopic

measure of network connectivity. A high average degree indicates that nodes are typically connected to many other nodes, suggesting robust propagation or efficient information exchange within the network.

Modularity, a key metric for evaluating the quality of network community structures, measures the degree of node clustering within communities. High modularity indicates a pronounced community structure, where nodes are more likely to connect with others in the same community rather than external ones. In urban traffic networks, areas with high modularity often correspond to regions with concentrated internal traffic flows, which can serve as indicators of high-traffic zones or regions requiring targeted transportation strategies. The modularity in a network is usually defined by the following formula proposed by Newman [38]:

$$L = \frac{1}{2m} \sum_{ij} \left[ A_{ij} - \frac{k_i k_j}{2m} \right] \sigma(c_i, c_j) \quad (4)$$

where,  $A_{ij}$  represents the adjacency matrix of the network,  $k_i$  and  $k_j$  denote the degrees of nodes  $i$  and  $j$ , respectively, and  $m$  is the total number of edges in the network. The summation is taken over all node pairs  $(i, j)$ . The function  $\delta(c_i, c_j)$  is an indicator function that equals 1 if nodes  $i$  and  $j$  belong to the same community (i.e.,  $c_i = c_j$ ), and 0 otherwise.

The network community metrics presented in Table 27, derived from the community structures identified using the Louvain algorithm, highlight the characteristic differences between the high- and low-frequency passenger networks during the first and second weeks. These metrics offer valuable insights into the behavioral patterns of high- and low-frequency passengers, reflecting how their travel preferences and interactions shape the community structures within the urban transportation network.

**Table 27.** Each network community indicator.

Network	Community	Size	Average Degree	Modularity
01high	1	112	35.51785714	0.176978184
	2	134	41.3880597	0.176978184
	3	48	20.33333333	0.176978184
	4	47	17.74468085	0.176978184
	5	14	7.428571429	0.176978184
	6	57	22.21052632	0.176978184
02high	1	28	21.07142857	0.224282329
	2	96	33.1875	0.224282329
	3	51	14.54901961	0.224282329
	4	157	41.41401274	0.224282329
	5	68	27.23529412	0.224282329
	6	14	7.857142857	0.224282329
	7	2	1	0.224282329
01low	1	122	44.85245902	0.210709338
	2	43	18.55813953	0.210709338
	3	46	19.34782609	0.210709338
	4	2	1	0.210709338
	5	19	12.21052632	0.210709338
	6	161	49.83850932	0.210709338
	7	38	15.68421053	0.210709338
02low	1	53	20.64150943	0.224288522
	2	89	30.92134831	0.224288522
	3	17	14.35294118	0.224288522
	4	131	36.33587786	0.224288522
	5	75	24.50666667	0.224288522
	6	50	20.56	0.224288522
	7	2	1	0.224288522

For high-frequency networks, the larger community sizes likely represent major routes used for daily commuting, while the higher average degree of communities (42) indicates

frequent passenger exchanges between stations. This suggests that high-frequency passengers tend to use diverse paths, reflecting a more varied travel pattern. The relatively low modularity (0.40) implies that these communities are not isolated clusters but are situated at critical intersections within the transportation network, allowing for greater flexibility in passenger flow across different communities.

In low-frequency passenger networks, the higher modularity (0.44) indicates more distinct community divisions. This strong internal connectivity may result from the occasional clustering of passengers for specific activities, such as weekend leisure or holiday events, leading to concentrated flows in certain areas. Larger community sizes may correspond to hotspots like tourist attractions or significant service points, which draw centralized traffic.

Urban planners can use these findings to tailor traffic planning strategies to the needs of different passenger groups. For high-frequency passengers, enhancing network connectivity and capacity is crucial, as their travel needs focus on daily, cross-district commuting with diverse paths. Improving network reliability and alleviating congestion in large high-frequency communities will directly enhance travel efficiency. This could involve allocating more public transport resources and increasing service frequency in key areas of high-frequency networks.

For low-frequency passengers, particularly within large communities, ensuring high-quality transportation services is vital to improve their travel experience. Strategies might include optimizing direct services to popular destinations and providing sufficient network capacity to accommodate sudden spikes in demand.

Overall, the mean and modularity indicators in high-frequency networks underscore the importance of inter-community mobility and flexibility in traffic planning, while the same metrics in low-frequency networks highlight the need to focus on destination-centric traffic and intra-community travel demands. This dual approach is critical for designing peak and off-peak transportation strategies that enhance both the efficiency of urban transportation systems and passenger satisfaction.

### 5.5. Analysis of Network Characteristics During Peak Hours

By integrating the cluster site information obtained earlier with the traffic data from the morning and evening peak periods, detailed traffic patterns at the stations are derived. This combined analysis, as shown in Tables 28 and 29, offers valuable insights into station-level traffic dynamics during peak hours. The results highlight the spatial and temporal distribution of passenger flows across different clustered stations, enabling a deeper understanding of network activity and passenger behavior during critical time periods.

Tables 30 and 31 illustrate the basic characteristics of the high- and low-frequency passenger networks, derived using consistent data analysis methods. These tables provide a detailed comparison of the structural and functional features of the networks, offering insights into their connectivity and passenger flow dynamics.

**Table 28.** Inter-station traffic after the morning rush hour passenger network in the first week.

Start-Site Node ID	Terminating-Site Node ID	Start-Site Longitude	Start-Site Latitude	Terminating-Site Longitude	Terminating-Site Latitude	Flow	Standardized Traffic
42	121	116.6307111	39.89759435	116.453518	39.9081348	10,617	0.742170022
42	234	116.6307111	39.89759435	116.470691	39.91255031	8381	0.585850112
234	121	116.470691	39.91255031	116.453518	39.9081348	6480	0.452950224
154	121	116.6583586	39.88788831	116.453518	39.9081348	5384	0.3763283
473	134	116.5270448	39.87229261	116.4986155	39.89621113	5227	0.365352349

**Table 29.** Inter-station traffic after the evening rush hour passenger network in the first week.

Start-Site Node ID	Terminating-Site Node ID	Start-Site Longitude	Start-Site Latitude	Terminating-Site Longitude	Terminating-Site Latitude	Flow	Standardized Traffic
121	42	116.453518	39.9081348	116.6307111	39.89759435	8312	0.581026286
121	234	116.453518	39.9081348	116.470691	39.91255031	6307	0.440855705
234	42	116.470691	39.91255031	116.6307111	39.89759435	5248	0.36682047
234	154	116.470691	39.91255031	116.6583586	39.88788831	5219	0.29488255
470	42	116.489658	39.91021268	116.6307111	39.89759435	4162	0.290897651

**Table 30.** Basic feature values of morning-peak network.

Networks	Global Agglomeration Coefficient	Mean Shortest Path	Network Efficiency
01high	$1.44388 \times 10^{-7}$	$1.41919 \times 10^{-5}$	10,179.60573
02high	$1.10448 \times 10^{-7}$	$6.93728 \times 10^{-6}$	10,827.55082
01low	$2.26735 \times 10^{-7}$	$8.59107 \times 10^{-6}$	10,313.71482
02low	$2.51985 \times 10^{-7}$	$1.01485 \times 10^{-5}$	9771.539936

**Table 31.** Basic feature values of evening-peak network.

Networks	Global Agglomeration Coefficient	Mean Shortest Path	Network Efficiency
01high	$1.44388 \times 10^{-7}$	$1.41919 \times 10^{-5}$	10,179.60573
02high	$1.10448 \times 10^{-7}$	$6.93728 \times 10^{-6}$	10,827.55082
01low	$2.26735 \times 10^{-7}$	$8.59107 \times 10^{-6}$	10,313.71482
02low	$2.51985 \times 10^{-7}$	$1.01485 \times 10^{-5}$	9771.539936

Among the network characteristics during peak periods, the average agglomeration coefficient for both high-frequency and low-frequency networks in the morning and evening peaks is significantly reduced compared to the overall period, with a decrease of 99%, particularly in high-frequency networks. This suggests that during peak hours, the travel network becomes more streamlined, reflecting passengers' need for direct routes, particularly among high-frequency commuters returning home from work.

Regarding the shortest path, the shortest path during peak times increases by approximately 10%. The high-frequency network exhibits a longer average path length, reflecting more inter-node connections during morning rush hours, while low-frequency passengers experience shorter and simpler travel routes. During the evening peak, however, the average path length becomes relatively short for both networks, indicating less detour and more direct travel paths.

Network efficiency analysis shows a 6% decrease in network efficiency for both high-frequency and low-frequency networks during the morning peak, while evening peaks exhibit relatively low efficiency for both. This decline likely results from commuters returning home, with complex paths and congestion reducing the overall efficiency of the transportation network.

High-frequency networks show a median node degree of 95 and an average of 158, with a heavy reliance on central nodes. Removing these nodes reduces network efficiency by 5% and the agglomeration coefficient by 0.1%. In contrast, low-frequency networks, with a median node degree of 110 and an average of 118, are more robust, maintaining structural integrity even after central node removal.

The global agglomeration coefficient is slightly higher in high-frequency networks (0.0009679085) than in low-frequency ones (0.0008830120). High-frequency networks exhibit more dispersed and complex travel patterns, leading to longer paths (16% increase) and reduced efficiency (5% decrease). Low-frequency networks, by comparison, have tighter structures and stronger inter-site connections, reflecting concentrated travel behavior.

### 5.6. Summary

Community analysis shows high-frequency networks have lower modularity (0.40) and higher inter-community mobility, while low-frequency networks exhibit higher modularity (0.44), often forming around specific activities or destinations.

Peak periods further emphasize network challenges, with a 99% drop in the agglomeration coefficient, a 10% increase in path length, and a 70% decline in efficiency. High-frequency networks experience greater congestion, with 30% longer paths and 6% lower efficiency during evening peaks compared to low-frequency networks.

Recommendations include enhancing central node capacity and decentralizing traffic in high-frequency networks, while improving accessibility and direct connections in low-frequency networks to boost utilization and efficiency.

## 6. Discussion

### 6.1. Policy and Research Implications

This study offers a comprehensive framework for analyzing urban public transit systems from a frequency-differentiated behavioral perspective. Unlike previous studies that treat the transit network as a homogenous flow system, this work reveals how high- and low-frequency passengers create fundamentally different spatial and structural footprints within the same infrastructure. The introduction of dual-mode flow networks, clustering of 53,000+ stations, and the mapping of community modularity and efficiency metrics across frequency groups represent methodological advances in multimodal network analysis. The integration of smart card and AVL data at this scale and granularity provides a foundation for scalable and transferable network vulnerability diagnostics. These findings help bridge the gap between human mobility behavior and complex network topology, contributing to the development of behavior-aware and resilient public transport strategies.

**Policy Implications and Targeted Interventions:** the results of this study yield actionable insights for urban transport planning and congestion mitigation. Key policy implications include:

- Peak-hour intervention. The observed 70% drop in network efficiency and 99% decline in clustering coefficient during peak periods highlight the urgency for congestion-mitigation strategies. Policymakers should consider targeted interventions such as dynamic pricing, staggered work shifts, or adaptive service scheduling to alleviate peak load stress.
- Enhancing robustness in high-frequency networks. The centralized and fragile structure of HF traveler sub-networks suggests a need for improving transfer hubs, reinforcing alternative paths, and adding redundant connections to reduce sensitivity to disruptions.
- Promoting accessibility in low-frequency networks. LF networks are more dispersed yet robust. Policies should focus on enhancing local connectivity, especially to peripheral destinations or leisure nodes. This could include adding feeder lines or integrating flexible microtransit services.
- Equity-aware planning. Given that LF passengers often include elderly, tourists, or irregular users, improving accessibility and service visibility in these communities

may enhance the inclusiveness of the network. The modular structures identified in LF communities support the design of localized, context-sensitive interventions.

- Future-ready infrastructure design. The analytical framework developed in this study enables simulation and scenario testing. By adjusting frequency thresholds or demand assumptions, planners can forecast network stress under projected growth or policy shifts, making the framework suitable for long-term resilience planning.

Overall, this work establishes a new analytical lens for public transport systems by fusing network science with frequency-based behavior modeling. Its implications extend beyond Beijing and can be generalized to other megacities adopting smart card systems and dual-mode transit networks.

## 6.2. Limitations and Future Work

While this study provides a comprehensive analysis of high- and low-frequency passenger networks in Beijing's transit system, several limitations must be acknowledged, along with promising directions for future research.

### 6.2.1. Threshold Selection for Passenger Frequency Classification

A key limitation of this study lies in the fixed threshold used to define high-frequency passengers—specifically, the top 25% of individuals ranked by weekly travel frequency. While this approach is inspired by practices in the air travel sector [39], where frequent flyer programs commonly adopt such percentile-based thresholds, it remains somewhat arbitrary in the context of urban public transportation, which lacks an established standard for frequency-based passenger classification.

In future research, more data-driven and statistically grounded methods should be explored to improve the robustness of this classification. This may include testing multiple threshold levels (e.g., top 10%, 20%, 30%) and comparing their impacts on network metrics and passenger behavior patterns. Moreover, the current binary segmentation into HF and LF passenger groups could be extended to multi-level classifications (e.g., three or five categories), allowing for a more nuanced understanding of intermediate-frequency user behavior. Unsupervised learning approaches or distribution-based segmentation—such as Gaussian Mixture Models [40] or histogram-based clustering—may help identify natural frequency groupings within the population. Such refinements would improve the interpretability, policy relevance, and generalizability of frequency-based transit analyses.

### 6.2.2. Scalability of Optimization Techniques

Due to the complexity and size of the Beijing transit network—encompassing over 53,000 stations and tens of millions of smart card records—this study focuses on structural diagnosis and simulation-based robustness analysis rather than solving a traditional optimization problem. We define the transit network as a weighted directed graph  $G = (V, E, W)$ , where:

- $V$  represents clustered station nodes;
- $E$  denotes directional edges representing passenger flows;
- $W$  indicates normalized traffic weights.

The network performance is evaluated via topological indicators such as global efficiency  $E_g$ , average path length  $L$ , clustering coefficient  $C$ , and modularity  $Q$ , which serve as proxy objectives. The structural vulnerabilities identified in high-frequency networks—such as centralized flow, long average path lengths, and low modularity—suggest several promising optimization directions.

To formalize this, we propose a future optimization framework where the goal is to enhance network robustness or efficiency while adhering to real-world constraints.

Specifically, the network  $G = (V, E, W)$  can be optimized via small structural modifications (e.g., adding or reinforcing edges), which leads to the following formulation:

$$\min_{G'} \Delta E(G, G') \quad \text{or} \quad \max_{G'} R(G') \quad \text{subject to budget and feasibility constraints}$$

Here,  $\Delta E(G, G')$  represents the change in efficiency before and after intervention, and  $R(G')$  is the robustness of the updated network  $G'$ . The feasible set of networks  $\mathcal{G}$  is constrained by practical considerations such as limited budget, maximum allowable number of added links, or equity requirements for coverage.

Even though this study does not solve the above optimization problem directly, our structural analysis provides the necessary groundwork: the identification of critical nodes, sensitivity of global metrics to disruptions, and areas with suboptimal flow or low redundancy. These insights can guide future algorithmic optimization efforts that search for the best set of edges to add or reinforce—thereby maximizing robustness or efficiency under real-world limits.

In addition to informing structural interventions under current conditions, this framework is also adaptable to future planning scenarios. For example, if projected changes in demand, route reconfigurations, or infrastructure expansions are available, they can be incorporated into the network  $G$  or its edge weights  $W$  to simulate and evaluate their potential impact on robustness and efficiency metrics. This allows the framework to serve as a forward-looking decision-support tool, capable of testing hypothetical scenarios and guiding policy decisions under varying future conditions.

Potential solution approaches could draw from combinatorial optimization (e.g., greedy heuristics, integer programming), spectral graph theory (e.g., maximizing algebraic connectivity), or reinforcement learning (e.g., environment-aware edge selection). In large-scale networks like Beijing's, these tools may enable data-driven, scalable transit planning.

#### 6.2.3. Passenger Demographics and User Profiling

One of the key limitations of this study is the lack of demographic information—such as age, occupation, and income level—with the available smart card dataset. While the dataset provides extensive spatiotemporal coverage and detailed travel chain information, it does not include personally identifiable or socioeconomic attributes of individual passengers due to privacy and data protection constraints.

As a result, we are unable to assess whether the sample distribution reflects the true population structure of urban transit users. For example, without knowing the proportion of commuters versus students or elderly passengers, there may be hidden sample biases that affect the interpretation of travel frequency patterns or network usage behaviors.

In future work, we aim to integrate complementary data sources (e.g., household travel surveys, census data, or anonymized demographic profiles provided by transit agencies) to perform passenger segmentation based on age group, employment status, and travel purpose. This will enable us to evaluate potential sampling biases more rigorously and analyze how network usage varies across demographic groups. Such insights are crucial for developing equitable and targeted transportation policies.

#### 6.2.4. Modeling Induced Demand Effects

An important direction for future work involves the incorporation of induced demand effects. As highlighted by Wiseman (2024) [41], improvements to transportation infrastructure—whether through physical expansion or enhanced service reliability—can lead to increased travel demand, potentially offsetting intended congestion relief [42]. Although the current study focuses on evaluating structural robustness and passenger

behavior within existing networks, future transit optimization strategies (e.g., route reallocation, increased capacity) may themselves trigger behavioral feedback loops.

To improve the long-term validity of policy recommendations, future models should consider integrating demand elasticity and behavioral adaptation components. This would allow for simulation of dynamic responses to network changes and better reflect real-world travel behavior under induced demand scenarios.

## 7. Conclusions

This study presents a comprehensive framework for analyzing urban public transportation networks through the lens of passenger travel frequency, utilizing over 20 million smart card records from Beijing's multimodal transit system. By constructing and comparing complex networks for high-frequency (HF) and low-frequency (LF) travelers, we uncover critical differences in spatial patterns, structural characteristics, and network resilience.

High-frequency passengers are predominantly concentrated in central urban areas and exhibit strong temporal clustering during morning and evening peaks. In contrast, low-frequency passengers demonstrate more dispersed spatial coverage and temporally flexible travel behaviors, reflecting distinct usage patterns. From a network topology perspective, HF networks display higher median (95) and average (158) node degrees, suggesting dense connectivity. However, they also exhibit reduced robustness, including a 0.5% drop in efficiency and a 0.1% decrease in clustering coefficient, compared to LF networks. The latter, while more fragmented, maintain greater structural stability and stronger intracommunity cohesion.

Community detection using the Louvain algorithm reveals further divergence. HF networks exhibit lower modularity (0.40) but higher average node degrees (42), resulting in tightly interlinked but fragile clusters. Conversely, LF networks demonstrate higher modularity (0.44) and lower average degrees (40), forming more distinct, stable communities often aligned with specific trip purposes or destinations. These structural characteristics have direct implications for network performance during peak periods. Under peak-hour conditions, the system experiences a 70% decline in efficiency and a 99% drop in clustering coefficient. The average path length increases by 10%, with HF networks specifically experiencing 30% longer paths and 6% lower efficiency than LF networks—highlighting their higher congestion sensitivity.

Building on these findings, we propose differentiated policy strategies. For HF networks, it is essential to reinforce network robustness through added redundancy, decentralize high-load hubs, and improve transfer environments. For LF networks, improving intra-community accessibility and ensuring equitable service to dispersed destinations can enhance overall system inclusivity. These targeted interventions support resilience, operational efficiency, and fairness in urban transit planning.

This research contributes to the field in several ways. First, it introduces frequency-based passenger segmentation into large-scale public transportation analysis, revealing how behavioral heterogeneity shapes network load and structural vulnerability. Second, it integrates smart card and AVL data into a scalable analytical framework that bridges micro-level behavior with macro-level topology. Third, it lays the foundation for future optimization studies by identifying critical nodes, fragile links, and flow imbalances—key targets for constraint-aware network enhancement.

Future research could further refine passenger classification through unsupervised learning or statistical modeling, explore the sensitivity of network properties under different frequency thresholds, and simulate long-term planning scenarios involving demand shifts, infrastructure expansion, or the transition to electric mobility. Incorporating weighted

station importance—e.g., prioritizing transfer hubs or capacity nodes—may also yield more nuanced insights into network flow patterns and planning priorities.

In summary, this study offers both theoretical and practical advances in understanding how different user groups shape the structure, efficiency, and vulnerability of large-scale urban transit systems. The proposed framework not only enhances our diagnostic capabilities but also informs forward-looking strategies to design more adaptive, inclusive, and resilient transportation infrastructures.

**Author Contributions:** Conceptualization, L.S. and M.P.; methodology, L.S.; software, L.S.; validation, L.S. and N.A.; formal analysis, L.S.; investigation, L.S.; data curation, L.S.; writing—original draft preparation, L.S.; writing—review and editing, L.S., N.A., and M.P.; visualization, L.S.; supervision, L.S., N.A., and M.P.; project administration, L.S., N.A., and M.P. All authors have read and agreed to the published version of the manuscript.

**Funding:** This research received no external funding.

**Data Availability Statement:** Processed data and visualization scripts are available at <https://github.com/lilieason/Transit-Network-Visual> (accessed on 3 August 2025). Raw data are not publicly available due to data provider restrictions.

**Acknowledgments:** We extend our appreciation to the research community and transportation authorities for making smart-card data and related infrastructure available for academic studies.

**Conflicts of Interest:** The funders had no role in the design of the study; in the collection, analyses, or interpretation of data; in the writing of the manuscript; or in the decision to publish the results.

## Abbreviations

The following abbreviations are used in this manuscript:

HF	High-Frequency (Passengers)
LF	Low-Frequency (Passengers)
AFC	Automated Fare Collection
AVL	Automated Vehicle Location
OD	Origin-Destination
EB	Electric Bus
WCSS	Within-Cluster Sum of Squares
SCC	Strongly Connected Component
GMM	Gaussian Mixture Model
TDA	Topological Data Analysis
RL	Reinforcement Learning
GIS	Geographic Information System
MRT	Mass Rapid Transit
CN	Community Network

## Appendix A. Interactive Visualization Links

To enhance readability and support dynamic exploration, all interactive versions of key visualizations presented in the manuscript are provided below:

**Table A1.** Supplementary links to interactive transit network visualizations corresponding to major figures in the manuscript.

Figure/Section	Interactive Visualization Link
Figures 6 and 7: Flow of OD pairs	<a href="https://github.com/lilieason/Transit-Network-Visual/tree/lilieason-patch-peakhour">https://github.com/lilieason/Transit-Network-Visual/tree/lilieason-patch-peakhour</a> (accessed on 3 August 2025)
Figures 9 and 10: Morning and evening peak flow (HF vs. LF)	<a href="https://github.com/lilieason/Transit-Network-Visual/tree/lilieason-patch-peakhour">https://github.com/lilieason/Transit-Network-Visual/tree/lilieason-patch-peakhour</a> (accessed on 3 August 2025)
Figures 11 and 12: Standardized heatingmap flow comparisons	<a href="https://github.com/lilieason/Transit-Network-Visual/tree/lilieason-patch-heatingmap">https://github.com/lilieason/Transit-Network-Visual/tree/lilieason-patch-heatingmap</a> (accessed on 3 August 2025)
Figures 16 and 17: Community detection and inter-community flow	<a href="https://github.com/lilieason/Transit-Network-Visual/tree/lilieason-patch-community">https://github.com/lilieason/Transit-Network-Visual/tree/lilieason-patch-community</a> (accessed on 3 August 2025)

## References

1. Litman, T. *Evaluating Public Transit Benefits and Costs*; Victoria Transport Policy Institute: Victoria, BC, Canada, 2015.
2. Derrible, S.; Kennedy, C. The complexity and robustness of metro networks. *Phys. Stat. Mech. Its Appl.* **2010**, *389*, 3678–3691. [[CrossRef](#)]
3. Yu, W.; Chen, J.; Yan, X. Space-time evolution analysis of the Nanjing metro network based on a complex network. *Sustainability* **2019**, *11*, 523. [[CrossRef](#)]
4. Sari Aslam, N.; Barros, J.; Lin, H.; Murcio, R.; Bei, H. Alighting location estimation from public transit data: A case study of Shenzhen. *Transp. Plan. Technol.* **2024**, *48*, 937–952. [[CrossRef](#)]
5. Shafiee, A.; Rastegar Moghadam, H.; Merikhipour, M.; Lin, J. Analyzing post-pandemic remote work accessibility for equity through machine learning analysis. In Proceedings of the International Conference on Transportation and Development 2024, Atlanta, GA, USA, 15–18 June 2024; pp. 453–462.
6. Ma, X.; Wu, Y.J.; Wang, Y.; Chen, F.; Liu, J. Mining smart card data for transit riders' travel patterns. *Transp. Res. Part Emerg. Technol.* **2013**, *36*, 1–12. [[CrossRef](#)]
7. Hounsell, N.B.; Shrestha, B.P.; D'Souza, C. September. Using automatic vehicle location (AVL) data for evaluation of bus priority at traffic signals. In *IET and ITS Conference on Road Transport Information and Control (RTIC 2012)*; IET: Stevenage, UK, 2012; p. 21.
8. Khanmohammadioustani, S.; HassanzadehKermanshahi, K.; Mohammadi, A.; Kermanshahi, S. Evaluating acceptance of a more strict plate control policy among motorcycle riders in Tehran. *Int. J. Transp. Eng.* **2023**, *11*, 1301–1311.
9. Chen, X.; Dai, X. Collection, analysis and application of bus IC card information. *China Civ. Eng. J.* **2004**, *37*, 105–110.
10. Dai, X. Research on Bus Data Analysis Methods Based on Bus IC Information. Ph.D. Thesis, Southeast University, Nanjing, China, 2006.
11. Dai, X.; Chen, X.; Li, W. Data mining techniques for bus IC card information processing. *Transp. Comput.* **2006**, *24*, 40–42.
12. Zhu, L. Design and implementation of a GIS-based spatio-temporal data model for bus planning. *Transp. Comput.* **2006**, *24*, 37–40.
13. Florida Department of Transportation. *APTS Data Archiving and Mining System (ADAMS)*; Final Report No. BD-549-31; Public Transit Office, Florida Department of Transportation: Tallahassee, FL, USA, 2007. Available online: <https://www.fdot.gov/transit> (accessed on 12 September 2024).
14. Barry, J.J.; Freimer, R.; Slavin, H. Use of entry-only automatic fare collection data to estimate linked transit trips in New York City. *Transp. Res. Rec. J. Transp. Res. Board* **2009**, *2112*, 53–61. [[CrossRef](#)]
15. Zhao, J. Estimating rail passenger origin-destination matrix using automatic data collection systems. *J.-Comput.-Aided Civ. Infrastruct. Eng.* **2007**, *22*, 376–387. [[CrossRef](#)]
16. Guerrero-Ibáñez, J.; Zeadally, S.; Contreras-Castillo, J. Sensor Technologies for Intelligent Transportation Systems. *Sensors* **2018**, *18*, 1212. [[CrossRef](#)]
17. Chen, T. Research on Commuter Travel Behavior Characteristics and Analysis Methods. Ph.D. Thesis, Beijing Jiaotong University, Beijing, China, 2007.
18. Xiao, F.; Xu, J.; Yang, L.; Liu, J.; Xue, L. Analysis and Application of Bus Travel Characteristics of Kunshan Residents Based on IC Card and GPS Data. In Proceedings of the Annual Conference on Urban Planning Informatization of China 2019: Smart Planning, Ecological Living, and High-Quality Space, Shenzhen, China, 15 November 2019; pp. 287–294.
19. Wen, Y.; Yan, K.; Cheng, F. Forecasting model of urban passenger transport hub transfer demand based on travel chains. *Transp. Transp. (Acad. Ed.)* **2005**, *1*, 1–3.

20. Dong, Y. Research on Prediction of Commuter Activity Arrangements. Ph.D. Thesis, Jilin University, Changchun, China, 2011.
21. Ali, A.; Kim, J.; Lee, S. Travel behavior analysis using smart card data. *KSCE J. Civ. Eng.* **2016**, *20*, 1532–1539. [CrossRef]
22. Viallard, A.; Trépanier, M.; Morency, C. Assessing the evolution of transit user behavior from smart card data. *Transp. Res. Rec.* **2019**, *2673*, 184–194. [CrossRef]
23. Kieu, L.M.; Bhaskar, A.; Chung, E. Passenger segmentation using smart card data. *IEEE Trans. Intell. Transp. Syst.* **2015**, *16*, 1537–1548. [CrossRef]
24. Wong, H.; Yap, M. A data-driven approach to update public transport service elasticities. *J. Public Transp.* **2023**, *25*, 100066. [CrossRef]
25. Wu, J. *Urban Transportation Systems Complexity: Complex Network Methods and Applications*; Science Press: Beijing, China, 2010.
26. Yan, H. Research on Urban Slow Traffic Network Characteristics Based on Complex Network Theory. Ph.D. Thesis, Chang'an University, Xi'an, China, 2012.
27. Wang, Z.; Chan, A.P.C.; Yuan, J.; Xia, B.; Skitmore, M.; Li, Q. Recent advances in modeling the vulnerability of transportation networks. *J. Infrastruct. Syst.* **2014**, *21*, 06014002. [CrossRef]
28. Bona, A.A.D.; Fonseca, K.V.O.; Rosa, M.O.; Lüders, R.; Delgado, M.R.B.S. Analysis of Curitiba's public transport system as a complex network. *Adv. Transdiscipl. Eng. Crossing Boundaries* **2016**, *4*, 267–276.
29. Yap, M.; Cats, O. Predicting disruptions and their passenger delay impacts for public transport stops. *Transp. Res. Part Policy Pract.* **2021**, *48*, 1703–1731. [CrossRef]
30. Wenz, K.P.; Serrano-Guerrero, X.; Barragán-Escandón, A.; González, L.G.; Clairand, J.M. Route prioritization of urban public transportation from conventional to electric buses: A new methodology and a study of case in an intermediate city of Ecuador. *Renew. Sustain. Energy Rev.* **2021**, *148*, 111215. [CrossRef]
31. Chen, S.; Piao, L.; Zang, X.; Luo, Q.; Li, J.; Yang, J.; Rong, J. Analyzing differences of highway lane-changing behavior using vehicle trajectory data. *Phys. Stat. Mech. Appl.* **2023**, *624*, 128980. [CrossRef]
32. Zhou, S.; Zang, X.; Yang, J.; Chen, W.; Li, J.; Chen, S. Modelling the coupling relationship between urban road spatial structure and traffic flow. *Sustainability* **2023**, *15*, 11142. [CrossRef]
33. Lyu, H.; Wu, J.; Zhang, J.; Gao, M.; Xu, W. Measuring urban road efficiency using trajectory data and complex network theory: A function-oriented approach. *Transp. Res. Part Emerg. Technol.* **2023**, *147*, 104004.
34. Ma, Y. Individual Travel Prediction Based on Clustering of Conventional Bus Passenger Travel Patterns. Ph.D. Thesis, Southwest Jiaotong University, Chengdu, China, 2022.
35. Azadeh, A.; Fekri, M.; Asadzadeh, S.M.; Barazandeh, B.; Barrios, B. A unique mathematical model for maintenance strategies to improve energy flows of the electrical power sector. *Energy Explor. Exploit.* **2016**, *34*, 19–41. [CrossRef]
36. Fekri, M.; Barazandeh, B. Designing an optimal portfolio for Iran's stock market with genetic algorithm using neural network prediction of risk and return stocks. *arXiv* **2019**, arXiv:1903.06632.
37. Barazandeh, B.; Curtis, K.; Sarkar, C.; Sriharsha, R.; Michailidis, G. On the convergence of Adam-type algorithms for solving structured single node and decentralized min-max saddle point games. In Proceedings of the ICASSP 2022–2022 IEEE International Conference on Acoustics, Speech and Signal Processing (ICASSP), Singapore, 23–27 May 2022; pp. 4343–4347.
38. Newman, M.E.J.; Girvan, M. Finding and evaluating community structure in networks. *Phys. Rev. E* **2004**, *69*, 026113. [CrossRef]
39. Betancourt, J.J.B. Air Time: Another Measure of the Quality of Passenger Service. Ph.D. Thesis, Massachusetts Institute of Technology, Cambridge, MA, USA, 2004.
40. Yang, M.S.; Lai, C.Y.; Lin, C.Y. A robust EM clustering algorithm for Gaussian mixture models. *Pattern Recognit.* **2012**, *45*, 3950–3961. [CrossRef]
41. Wiseman, Y. Autonomous vehicles will spur moving budget from railroads to roads. *Int. J. Intell. Unmanned Syst.* **2024**, *12*, 19–31. Available online: <https://u.cs.biu.ac.il/~wisemay/ijius2024.pdf> (accessed on 10 October 2024). [CrossRef]
42. Wu, J.H.; Nash, C. Railway reform in China. *Transp. Rev.* **2000**, *20*, 25–48. [CrossRef]

**Disclaimer/Publisher's Note:** The statements, opinions and data contained in all publications are solely those of the individual author(s) and contributor(s) and not of MDPI and/or the editor(s). MDPI and/or the editor(s) disclaim responsibility for any injury to people or property resulting from any ideas, methods, instructions or products referred to in the content.